

SAND DEPOSITION IN THE COLORADO RIVER IN GRAND CANYON FROM FLOODS IN THE LITTLE COLORADO RIVER

By Stephen M. Wiele, Julia B. Graf, and J. Dungan Smith

U.S. Geological Survey

**GCES OFFICE COPY
DO NOT REMOVE!**

Prepared in cooperation with the

Bureau of Reclamation

Boulder, Colorado
June 1995

500.03
PRT-10.00
C719
23359

-1-
2114 843 - predraft letter

216

CONTENTS—for review purposes only

	Page
Abstract.....	5
Introduction.....	6
Background	8
Approach	9
Pool Morphology and Processes.....	13
Estimated Little Colorado River Inflow	16
Field Measurements of Topography and Sand-Storage Changes	21
Channel Topography.....	21
Measured Cross Sections	23
Development of Interpolation Method.....	25
Grid Generation.....	25
Model Development.....	25
Flow Field	26
Sediment-Transport Field	30
Bed-Evolution	33
Application to the Little Colorado River Flood of January 1993	34
Comparison of Measured and Computed Changes at Monumented Cross Sections ..	35
Comparison of Preflood and Postflood Topography and Flow Fields in the Four Study Reaches.....	40
Computed Depositional Volumes and Rates of Sand Accumulation	40
Discussion	44
Summary and Conclusions	49
Acknowledgments.....	50
References.....	51

ILLUSTRATIONS—for review purposes only

	Page
Figure 1. Map showing the location of model reaches, measured cross sections, and streamflow gaging stations used in the study.....	11
2. Graph showing reconstructed instantaneous discharge at the mouth of the Little Colorado River and in the mainstem Colorado River downstream from the confluence during the flood of January 1993.....	22
3. Graph showing measured and computed cross sections A1-A5 from before and after the Little Colorado River flood of January 1993 for study reach 1.....	39
4. Graph showing measured and computed cross sections A6 and A7 from before and after the Little Colorado River flood of January 1993 for study reach 2.....	41
5. Graph showing measured and computed cross sections B2-B4 from before and after the Little Colorado River flood of January 1993 for study reach 3.....	43
6. Graph showing measured and computed cross sections C1-C5 from before and after the Little Colorado River flood of January 1993 for study reach 4.....	45
7. Graph showing the initial topography and flow field in model reach 1 (left) and the topography and flow field after 6 days (right).....	47
8. Graph showing the initial topography and flow field in model reach 2 (left) and the topography and flow field after 6 days (right).....	48
9. Graph showing the initial topography and flow field in model reach 3 (left) and the topography and flow field after 6 days (right).....	49
10. Graph showing the initial topography and flow field in model reach 4 (left) and the topography and flow field after 6 days (right).....	50
11. Graph showing the relation of sand volume computed by the model to time (top) and sand volume normalized by flow volume (bottom) for each of the four study reaches.....	53

12. Map showing the initial topography of model reach 4 with area defined as main channel, recirculation zones, and channel margins.....55
13. Graphs showing change in sediment volume (top) and rate of change of sediment volume (bottom) with time for the total area of model reach 4 and for areas defined as main channel, recirculation zones, and channel margins.....56
14. Graphs showing (A) the initial channel morphology and flow pattern for model reach 4 and the morphology and flow pattern 6 hours (B), 12 hours (C), 24 hours (D), 2 days (E), 3 days (F), 4 days (G), and 6 days (H) after the beginning of model simulation.....60

SAND DEPOSITION IN THE COLORADO RIVER IN GRAND CANYON FROM FLOODS IN THE LITTLE COLORADO RIVER

S. M. Wiele

Water Resources Division, U.S. Geological Survey, Boulder, Colorado

J. B. Graf

Water Resources Division, U.S. Geological Survey, Tucson, Arizona

J. D. Smith

Water Resources Division, U.S. Geological Survey, Boulder, Colorado

Abstract. Methods for computing the volume of sand deposited in the Colorado River in Grand Canyon National Park by floods in major tributaries and for determining redistribution of that sand by main-channel flows are required for successful management of sand-dependent riparian resources. We have derived multidimensional flow, sediment transport, and bed-evolution models based on a gridded topography developed from and adapted to measured channel topography and used these to compute deposition in a short reach of the river just downstream from the Little Colorado River, the largest tributary in the park. Model computations of deposition from a Little Colorado River flood in January 1993 were compared to bed changes measured at 15 cross sections. The total difference between changes in cross sectional area due to deposition computed by the model and the measured changes was 5.6 percent. Depositional volumes were found to depend sensitively on the morphology of the channel. A wide reach with large areas of recirculating flow and large depressions in the main channel accumulated the most sand whereas a reach with similar planimetric area but long, narrow shape and relatively small areas of recirculating flow and small depressions in the main channel accumulated only about a seventh as much sand. About 32 percent of the total deposition was in recirculation zones and 65 percent was in the main channel. Overall, about 15 percent of the total input of sediment from this Little Colorado River flood was deposited in the first 3 km below the confluence, suggesting that deposition of the flood-derived material extended for only several tens of kilometers downstream from the confluence.

Introduction

Closure of Glen Canyon Dam in 1963 turned a once abundant sand supply in the Colorado River through the Grand Canyon into a precious resource. Understanding the fate of sediment added to the Grand Canyon segment of the Colorado River from its two main sources, the Paria and Little Colorado Rivers, is crucial if the limited influxes of sand are to be managed to support a precarious riparian environment. Effective management of the river corridor for environmental purposes requires accurate methods to estimate (1) the volumes and distributions of sand contributed by floods on the two major tributaries and (2) the rates and patterns of redistribution of that sand by dam-regulated mainstem flows.

Flooding on the Little Colorado River in January 1993 significantly replenished the sand in the mainstem downstream from the confluence. Much of that sand restored deposits near the water surface along the channel edges. The remainder was deposited within the channel where it became a source of sand for enhanced downstream transport or a sand supply that could be redistributed to the channel edges by skillful and timely manipulation of dam releases. Effective redistribution of sand to the channel edges, however, requires keeping careful track of where the ever-moving sand mass is in the system.

Accurate evaluation of sand resources by direct measurements of the volumes of sand deposits using geophysical methods or by direct measurement of changes in sand distribution using dense topographic surveys is not feasible because of the large size of the system (380 km) and its inaccessibility, the high cost of making necessary field measurements, and the high degree of variability in channel geometry and sand storage. Consequently, a method that employs both field techniques and flow and sediment-transport modeling has been developed to estimate rates and volumes of sand deposition and erosion. This method combines multidimensional flow, sediment-transport, and bed-evolution modeling with measured bed and bank topography and a limited set of monitored topographic cross-sections. The method is used here to estimate volume and distribution of sand deposited in four 1/4-1/2 km reaches of the Colorado River below the Little Colorado River following a substantial flood on that major sand-contributing tributary in January 1993.

Background

By the early 1980s, agencies charged with management of the Colorado River in the Grand Canyon, white-water rafters, and anglers had become concerned that the mode of operation of Glen Canyon Dam was eroding sand bars critical to the riparian ecological system in Grand Canyon National Park. This concern prompted the Bureau of Reclamation (BOR) to initiate an investigation of the sand resources in the river between Lake Powell and Lake Mead, and since 1983, the BOR has coordinated a comprehensive program of investigations—the Glen Canyon Environmental Studies (GCES)—to determine the effects of releases from Glen Canyon Dam on the riparian and aquatic resources in the park. As part of GCES, the U.S. Geological Survey (USGS) began in 1989 to develop a suite of flow and sediment-transport models for predicting the response of sand in the canyon to dam releases. Reach-averaged, one-dimensional models are used for routing the unsteady flow and sand through the entire system, whereas multidimensional models are being used to investigate local phenomena of particular interest or importance.

Concern about sand bars has focused on their potential degradation by moderate to high amplitude unsteady flows resulting from power-plant releases and by prolonged high flows resulting from releases above power-plant capacity that occasionally are required to reduce the water level in Lake Powell. The presence of sand bars in the Grand Canyon depends on a complex interaction of channel morphology, sand supply, flow, and sediment transport. Accurate prediction of their response to dam-regulated flows within and above power-plant capacity is required to manage the system for minimum impact on downstream resources, while retaining adequate flexibility in dam operation.

Restrictions were placed on power-plant releases in 1992 because of growing concern over the effects of dam releases on riparian resources. The restrictions, called Interim Flow Criteria, set limits on maximum and minimum daily releases and on the rate of increase and decrease of releases and were in effect during the period of measurements used in this report. The daily mean discharge at Lees Ferry, Arizona, about 25 km downstream from the dam, was between about 200 and 500 m³/s, with the range in discharge during a given day commonly between about 100 and 200 m³/s.

Approach

The frequency and density of field measurements is severely limited by remoteness of the location, which translates into high cost, and by the need to limit intrusion into the fragile and valued riparian system of Grand Canyon National Park and into areas held sacred by Native Americans. As a result, we have made a limited number of field measurements designed to be used in conjunction with a model that provides a physically-based method of interpolating changes in bed topography both in time and space. The field measurements consist of initial bed topography from which the gridded model topography was developed and a limited number of cross sections that give accurate measurements of changes in bed elevation at a discrete set of times and locations.

A monitoring program was initiated in 1992 to provide information on the state of the riparian system under the restricted dam operating rules. As a part of the interim-flow monitoring program, the USGS established networks of monumented cross-sections downstream from the two largest tributaries, the Paria and Little Colorado Rivers, to determine the deposition volumes and patterns from tributary floods and the subsequent remobilization of sand supplied by these major sources (Figure 1). Fifteen of 32 sections in a network below the Little Colorado River were established and first measured in June-July 1992 (Figure 1). A period of high discharge that lasted about three weeks and included two floods of moderate peak discharge, about 500 and 300 m³/s, and durations of 5-6 days each, occurred on the Little Colorado River in January 1993. This period of high discharge contributed an estimated 4.17 Tg (about 4,600,000 tons) of sand to the Colorado River and caused aggradation of the bed at many of the cross sections downstream. These cross sections were remeasured in late January and early February 1993.

Previous work has shown that the bed of the Colorado River in Grand Canyon National Park is about 60 percent bedrock, talus blocks, or boulders and that sand brought to the river by tributary floods is temporarily stored in pools separated by rapids or in thin, commonly discontinuous layers over an immobile bed [Howard and Dolan, 1981; Wilson, 1986; Schmidt and Graf, 1990]. Monitoring sections were established at locations judged to be most likely to have the greatest amount of erosion and deposition. Bank characteristics and visible bed and channel geometries were the primary factors used to select cross-section locations, because the monitoring began before the topography was known, hence before our models could be used to identify appropriate monitoring sites. Measurements at the monumented sections, repeated about three times a year since their establishment, demonstrate that inflow of sand from the Little Colorado River and subsequent scour can produce changes ranging from 0-12 m in bed elevation at the measured sections [Graf et al., 1995b].

Figure 1. Location of model reaches, measured cross sections, and streamflow gaging stations used in the study.

Accurate characterization of channel geometry up to the highest elevation of expected flows is required for creation of the multidimensional models needed to estimate volume changes with reasonable accuracy. In 1989, a group of GCES scientists selected 13 reaches along the river corridor of 5-31 km in length for detailed topographic mapping and development of a geographic database. The database was developed by the BOR using ARC/INFO Geographic Information System (GIS) software [Environmental Systems Research Institute, Inc., 1991] and data are maintained by the BOR as ARC/INFO coverages. [Werth et al., 1993]. In 1991, the USGS began collection of bathymetric data for the reaches in the GIS database to extend the channel-morphology information to the channel bottom. The reach downstream from the Little Colorado River was selected to begin development of sand-volume estimation methods because of a high degree of interest in this reach by the GCES Office and other scientists, and because cross-section measurements made before and after the January 1993 flood provided an ideal data set with which to evaluate the approach.

The reach is of special interest because it is important to the survival of remaining native fish and because the Little Colorado River is the largest source of sand to the Colorado River in the Grand Canyon. The reach just below the Paria River is also important from a sand resource point of view, because virtually no sand is added to the system above this location, and as Paria River flood-produced sand deposits move downstream, the sand resources in this upper Marble Canyon reach become especially vulnerable to the mode of dam operation. A model similar to the one reported in this paper is under development for use in evaluating sand deposition and depletion in this sensitive region.

Multidimensional models of flow and sediment transport have been successfully implemented in geomorphology and engineering studies of bed evolution in natural rivers [e.g. Shimizu and Itakura, 1985; Shimizu et al, 1987; Nelson and Smith, 1989; Andrews and Nelson, 1989; Wiele, 1992]. Bennett [1993] developed and applied a one-dimensional flow and sediment-transport model to the Colorado River reach below the confluence with the Little Colorado River. The model developed in this study, like the multidimensional models referenced above, calculates the flow field for a given discharge using a gridded version of the measured bathymetry. The sediment-transport field is then calculated from the flow field and used to determine the change in bed morphology for a small time step. This process is repeated until the desired time period has been modeled. In this study, the model's fidelity is checked by comparing the predicted bed shape to the measurements at the monumented cross sections. Differences between the initial bed surface and calculated surfaces for later times can be used to determine rates of deposition, both for the reach as a whole and by depositional environment, and to determine total volumes of sand deposited.

Pool morphology and processes

In the Colorado River below the confluence with the Little Colorado River, pools of tranquil flow are bounded on the upstream and downstream ends by fans formed by debris flows and floods from streams in side canyons [Howard and Dolan, 1981; Schmidt, 1987; Schmidt and Graf, 1990, Webb et al., 1989]. Flow through the constrictions created by the fans that partially block the channel forms the well-known rapids of the Grand Canyon, in which flow is supercritical, slopes are steep, and boulders deposited by debris flows produce a high relative roughness [Kieffer, 1987]. The lengths of pools are determined by the spacings between debris fans, which, in turn, are controlled by bedrock structure to a large degree [Dolan et al., 1978]. In the reach below the Little Colorado River, the pools are typically 1/4-1/2 km long (Figure 1).

Lateral divergence of the flow into channel expansions results in deposition of sand along the channel margins. Lateral expansions that contribute most significantly to sand deposition form primarily in the lee of debris fans. Expansion ratios, the ratio of width of a pool to the width of the upstream rapid, in the 100 kilometer reach above the confluence with the Little Colorado River have a mean value of 2.9, and range from 1.3 to 7.3 [Schmidt and Graf, 1990]. Recirculation zones typically form in the lee of debris fans that produce the upstream boundaries of the pools. Sediment is deposited near the reattachment point of a recirculation zone by flow spreading from the main current. Some sediment is carried into the recirculation zone and deposited by other processes as discussed by Nelson et al. [1995]. Sand deposits within and adjacent to the recirculation zone have been described and classified by Schmidt and Graf [1990] as separation deposits, which form near the upstream part of the recirculation zone; reattachment deposits, which form upstream and downstream from the recirculation zone stagnation point; and eddy-center deposits. Rubin et al. [1990] described the details of the complex small-scale depositional processes, inferred from sedimentary structures.

Channel margin deposits also form near the banks of relatively straight parts of the channel apart from recirculation zones. The mechanics of the formation of these deposits have been investigated by Smith and Wiele [1994] who have proposed that the erosion or accumulation of these deposits depends on cross-stream sand-concentration gradients that are stage dependent. At high stages, sand tends to diffuse from the channel center to the margins where some of it is deposited, whereas at low stages density-driven cross-stream circulation and diffusion erodes sand from the channel margins and delivers it to the channel center.

Previous studies of sand deposition in the Grand Canyon have focused on deposition in recirculation zones because deposits are accessible for measurement and are important to both the riparian environment and to boaters, who use them as campsites. However, the main channel has the capacity to store significant amounts of sediment during tributary flooding, especially in the depressions typically worn into the bedrock just downstream from the rapids, depressions that can be as much as nine times deeper than the depth in the upstream rapid [Schmidt and Graf, 1990]. The divergence of the shear stress that results from the vertical expansion of flow into these depressions promotes deposition. Proposals to scour sediment from channel storage and place it along the margins using carefully designed periods of high steady discharge from Glen Canyon Dam [BOR, 1994] have recently received increased interest.

In the discussions that follow of the three depositional environments appropriate for the scale considered here, we adopt the nomenclature of Schmidt and Graf [1990]: main channel deposits are located within or near the thalweg where most of the water discharge is conveyed downstream, eddy-associated deposits are within the recirculation zone or are near the stagnation point, and channel margin deposits are in the low-velocity zones near the banks apart from the eddy-associated deposits.

The extent of sand on the bed in the main channel varies from complete coverage of sufficient thickness to form dune fields to partial coverage in which patches of sand are dispersed over a bedrock and gravel bed [Wilson, 1986; J.B. Graf, unpublished data; Roberto Anima, personal communication, USGS, Menlo Park, 1994]. The divergence of suspended-sediment discharge along streamlines depends on the boundary shear-stress divergence and the extent of coverage of the bed with suspendable sediment. Patchy sand distribution on the bed produces a lower near-bed concentration and, as a result, a lower suspended-sediment concentration in the water column than is produced when the bed is completely covered with sand. When no storm runoff is occurring in tributaries below Glen Canyon Dam, the Colorado River has low suspended-sediment concentration, and the low concentration causes the bed in the center of the channel to tend towards an equilibrium state in which the fraction of the bed covered by sand is such that the sediment capacity of the characteristic flow is constant along streamlines [Smith and Wiele, 1995]. The deeper, lower shear-stress parts of the channel will tend to have a higher percentage of the bed covered by sand than those parts of the main channel where the shear stress is higher. An influx of relatively high-concentration flow from a tributary flood to a channel adjusted to low-concentration dam releases leads to rapid deposition and blanketing of the bedrock and gravel bed with sand. Deposition will be most rapid in the depressions downstream from the constrictions, where the large increase in flow depth causes the greatest divergence of the boundary shear-stress.

Estimated Little Colorado River Inflow

Inflow of sand and water from the Little Colorado River to the study reach during the January 1993 flood was computed using records from streamflow-gaging stations on the Colorado River above and below the Little Colorado River confluence and on the Little Colorado River itself. Gaging stations on the Colorado River at Lees Ferry and near Grand Canyon (Figure 1) provided streamflow information used to estimate the unsteady water inflow from the Little Colorado River mouth, and two gaging stations on the Little Colorado River provided information for estimation of sand load delivered to the Colorado River during the flood.

The sand load carried by the flood of January 1993 was estimated from data from streamflow-gaging stations on the Little Colorado River at Grand Falls and near Cameron, 72 and 60 km upstream from the mouth, respectively (Figure 1). The downstream gaging station, near Cameron, is a USGS daily-sediment site and daily suspended-sediment and sand loads were estimated using standard USGS techniques [Gregory G. Fisk, U.S. Geological Survey, Flagstaff, Arizona, personal communication]. High river levels caused lost stage record at the gaging station near Cameron for much of the flood period, but the stage record at the Grand Falls gaging station covers the entire period. To compute sand load at the Cameron gaging station, daily mean discharge for the period January 7-29 was estimated from the record at the Grand Falls gaging station and a relation giving travel-time of runoff between the two sites developed from previous runoff periods [Gregory G. Fisk, U.S. Geological Survey, Flagstaff, Arizona, personal communication]. Daily sand load at the Cameron gaging station was determined using the estimated daily discharge and a relation between daily sand load and daily mean discharge developed with information from previous runoff periods. Flooding of an auxiliary pump on an automatic suspended-sediment sampler at the gaging station near Cameron caused failure of that sampler in the later part of the period, but some samples were collected before failure. Sand concentration in samples collected during the January flood was typical of winter runoff in the Little Colorado River basin and a relation developed for the winter period was used for the estimate. The sum of the estimated daily sand loads for the period January 7-29, 1993, is 4.17 Tg.

The flood hydrograph at the mouth of the Little Colorado River was calculated indirectly from hydrographs at the streamflow-gaging stations on the Colorado River at Lees Ferry, 100 km upstream from the Little Colorado River confluence, and near Grand Canyon, 42 km downstream from the confluence, using a one-dimensional diffusion wave model (1D model) of discharge waves released from Glen Canyon Dam developed by Wiele and Smith [1995] together with a kinematic-wave model that uses the same hydraulic geometry as the 1D model. The method consists of routing the hydrograph from the Lees Ferry gaging station downstream to the confluence using the 1D model, routing the hydrograph at the Grand Canyon gaging station upstream and backwards in time to the confluence with the kinematic-wave model, and computing the inflow hydrograph as the difference between the two.

For a kinematic wave, the momentum equation is simplified such that the shear stress is a function of only two channel properties: the ambient water-surface slope and the hydraulic radius [Lighthill and Whitham, 1955]. That form of the momentum equation is combined with the continuity equation to give:

$$\frac{\partial Q}{\partial t} + c_w \frac{\partial Q}{\partial x} = 0 \quad (1)$$

where:

Q	discharge
t	time
x	streamwise dimension
c_w	wave speed = dQ/dA
A	cross-sectional area

Because the phase speed of a kinematic wave is a function only of channel properties and not of the wave characteristics, the wave speed for a given point on a hydrograph can be determined from the discharge at that point, given the hydraulic geometry. The hydrograph at the confluence was determined from the hydrograph at the gaging station near Grand Canyon from (1) by calculating the time required for each point on the hydrograph to travel the distance between the confluence and the gaging station. The calculation of downstream hydrographs using this procedure is described by Chow et al. [1988]. The distance over which this method can be applied with reasonable accuracy is limited, however, by the absence of diffusion in the kinematic-wave model.

The small-scale fluctuations in the computed Little Colorado River hydrograph (Figure 2) are a result of small timing discrepancies between the two computed hydrographs, as well as of unsteadiness in the Little Colorado River inflow. The hydrograph of inflow to the study reach was computed by adding the computed Little Colorado River inflows at the confluence to the Colorado River discharges routed to the confluence from the Lees Ferry gaging station with the 1D model (Figure 2). Owing to the high degree of irregularity of the Colorado River channel and bed roughness, the geometric characteristics of the river must be averaged over a reach several tens of kilometers in extent before kinematic-wave theory can be applied to it. This averaging is required for discharge-wave routing because discharge waves are many tens of kilometers in length. The length of a discharge wave of a typical structure and daily period and ranging from 142 to 425 m³/s, for example, is about 200 km, and as it moves downstream all small-scale structures are averaged out.

Figure 2. Reconstructed instantaneous discharge at the mouth of the Little Colorado River and in the mainstem Colorado River downstream from the confluence during the flood of January 1993.

Field Measurement of Topography and Sand-Storage Changes

Channel Topography

Bathymetric data were collected in June-July 1992 with a manual-tracking range-azimuth positioning system that consists of a standard electronic theodolite to establish the ties to the control network and a modified laser electronic distance meter (EDM) mounted above the theodolite to track a target on the boat. Depth was measured with a sonic depthsounder, and digital position and depth data were sent via radio modems to a datalogger. Depth was also continuously recorded on paper charts. Surveys were made by crossing the channel at about 10 m intervals. Location and depth were recorded at 0.25 to 0.50 m intervals along the traverse lines. A more detailed description of the data and the methods of data collection and analysis is given by Graf et al. [1995a].

As a part of the GCES database effort, a vertical- and horizontal-control network in Arizona State Plane Coordinate System, in meters, using a Transverse Mercator projection was established for the reaches in the database. Topographic contours above a low-discharge (about 142 m³/s) river stage were developed photogrammetrically from aerial photographs taken in June and July 1990 and 1991 and stored as line coverages in the GCES GIS database [Werth et al., 1993]. The contour interval for these topographic data varies but is as small as 0.5 m in areas of relatively low relief.

After verification of position and depth data from bathymetric surveys, the positions of the data points were converted from the arbitrary x,y coordinate system in which they were collected into the Arizona State Plane coordinate system used in the GCES GIS database [Werth et al., 1993]. Depth data were converted to elevation using water-surface-elevation data collected at the time of the survey. Elevations of the surface defined by bathymetric surveys and the surface defined by the GCES topographic contours in areas of overlap were compared, and if significant difference was found, the topographic data were used to define the surface. This was done because the bathymetric data were sparse and less accurate near the edges of the channel, which typically was the overlap zone.

To generate a surface from which to compute a grid of equally-spaced data points, a network of triangles (TIN) was first created from points in the combined topographic and bathymetric data set using the Delaunay method of triangulation [McCullagh and Ross, 1980] as implemented by the ARC/INFO software. The high density of data points from the bathymetric surveys along traverse lines created a point distribution that produced a large number of very long, narrow triangles that gave unrealistic interpolated elevations. To produce a more equally-spaced point distribution and therefore a TIN with triangles that were more equilateral, the data were filtered to remove points within a given radius of the previous point. The point spacing that was found to produce the most realistic interpolated elevations was 4 m for these data sets. An interpolation algorithm using a bivariate fifth-degree polynomial in x and y [Akima, 1978] was used to compute elevations at grid points and contour-line positions from the network. During development, the interpolation scheme was evaluated for accuracy by comparison of contours computed by interpolation from the TIN to contours developed photogrammetrically for the topographic data set.

The ability of TIN and the interpolation scheme to represent the surface was also evaluated by examining the difference between measured and interpolated elevations of points not used to generate the TIN. For the data from model reach 1, for example, about 15 percent of the 10,212 data points was used to generate TIN and the remaining 8,681 data points were used for comparison of measured and computed elevations. No areal pattern was revealed when deviations of the measured elevation from the computed surface were plotted on a map of the study reach, and no bias or trends were shown by the relation of the deviations to elevation. For model reach 1, the mean deviation was only slightly different from zero (-0.28 m) and the standard deviation of the deviations was about 2 m. The frequency distribution of deviations is strongly unimodal, and 95 percent of the observations are between -2 and +2 m. The differences between measured and interpolated surfaces is a measure of the irregularity of the channel shape resulting from bedrock controls and bedforms. Form drag on these irregularities produces the primary friction on the flow.

Measured Cross Sections

Fifteen cross sections were established in the first few reaches downstream from the Little Colorado River confluence. Those were first measured in June-July 1992 at the time of the bathymetric survey and remeasured in late January through early February 1993, just after the January 1993 Little Colorado River flood (Figure 1). Methods of data collection and analysis for the cross-section measurements are described in detail by Graf et al. [1995b].

For each measurement, a line with flags at 6.1 m intervals was strung across the river between the section endpoints. A measurement is made up of 10 consecutive passes across the river under the line. Because depth differences over short distances can be large, a significant variation in measured depth at any position along the line was observed even with the use of a fixed line and with every effort to keep the boat under the line. The 10 passes were made to characterize the variability and define the mean section as accurately as possible. Each pass was digitized from the graphical record. Once the data were digitized, the distance of each point from the left bank reference point in inches of graph paper was converted to ground distance in meters using the known locations of the fix marks on the graphical record and assuming constant boat speed relative to the ground between marks. To provide depths at equal distances from the zero point, points were selected or interpolated at 0.25-m intervals across the channel. The number of values, the mean, median, and maximum and minimum depths, and standard deviation from the mean depth were computed for each distance from the zero point from the 10 passes that comprise a measurement. Cross-section measurements used for comparison to model results are the mean of the 10 passes.

Development of the Interpolation Method

Grid Generation

Grids for model computations were determined by first computing the x and y coordinates of the grid points in the coordinate system of the data from endpoints of the upstream boundary, the length of the grid, and the grid spacing in the x and y directions. A 10 by 10 m grid spacing was used for all computations discussed in this report. Elevation at each grid point was then computed from the TIN developed for the reach using the interpolation scheme described above. In some cases, extreme irregularities in the bedrock required additional smoothing, and in these cases the elevation at each grid point was averaged with the average of the 4 adjacent points to reduce the local irregularity.

Model Development

The Colorado River in the Grand Canyon is entrenched in bedrock and lined with immovable talus in many reaches, yet the channel is alluvial in some sections in that its shape is self-formed by gravel and sand. The sand is easily transported even at low discharge, but significant gravel transport occurs only at discharges exceeding the power-plant capacity of about 930 m³/s. The flow and sediment-transport model calculates sand transport in suspension, deposition, and erosion of sand within a channel shape fixed by bedrock and gravel.

The numerical part of the model can be divided into three calculation components: the flow field, the sediment transport field, and the bed evolution over time.

Flow Field. Calculation of the flow field consists of a numerical solution of the St. Venant equations for two-dimensional flow, momentum in the x direction:

$$\frac{\partial u}{\partial t} + u \frac{\partial u}{\partial x} + v \frac{\partial u}{\partial y} - \frac{\partial}{\partial x} \epsilon \frac{\partial u}{\partial x} - \frac{\partial}{\partial y} \epsilon \frac{\partial u}{\partial y} + g \left(\frac{\partial h + \eta}{\partial x} - S \right) + \frac{\tau_x}{\rho h} = 0 \quad (2)$$

momentum in the y direction:

$$\frac{\partial v}{\partial t} + v \frac{\partial v}{\partial y} + u \frac{\partial v}{\partial x} - \frac{\partial}{\partial y} \epsilon \frac{\partial v}{\partial y} - \frac{\partial}{\partial x} \epsilon \frac{\partial v}{\partial x} + g \frac{\partial h + \eta}{\partial y} + \frac{\tau_y}{\rho h} = 0 \quad (3)$$

and continuity:

$$\frac{\partial h}{\partial t} + \frac{\partial uh}{\partial x} + \frac{\partial vh}{\partial y} = 0 \quad (4)$$

where:

- x direction normal to the upstream boundary
- y direction normal to x
- t time
- u vertically-averaged velocity in the x direction
- v vertically-averaged velocity in the y direction
- h flow depth
- η bed-surface elevation
- S average reach slope
- ϵ eddy viscosity
- g gravity
- ρ density of water
- τ_x shear stress in the x direction
- τ_y shear stress in the y direction

The second-order terms generally are negligible in the converged solution, except for the cross-stream term near a bank, but they are retained because of their beneficial influence in promoting convergence.

The numerical method used to solve the flow equations follows the procedure described by Patankar [1980] for two-dimensional compressible conduit flow, with the substitution in the equations of motion of flow depth for density and use of the water-surface gradient in the pressure term. The method features a staggered grid for the u , v , and h components and upwind differencing.

The shear stress, τ , is related to the velocity by a friction coefficient, c_f :

$$\tau = \rho c_f U^2 \quad (5)$$

where U is the magnitude of the resolved velocity. The x and y components are determined from the relations:

$$\tau_x = \rho c_f u U \quad (6)$$

and

$$\tau_y = \rho c_f v U \quad (7)$$

The friction coefficient is defined as

$$c_f = \left(\frac{\kappa}{\ln \left(\frac{h}{z_0} - 1 \right)} \right)^2 \quad (8)$$

and is derived from the logarithmic velocity profile [Keulegan, 1938]:

$$u(z) = \frac{u_*}{\kappa} \left(\ln \frac{z}{z_0} \right) \quad (9)$$

where κ is von Karman's constant, z is the vertical direction, and z_0 is the roughness parameter, discussed in more detail below. Equation (9) permits an approximate solution of the three-dimensional flow field from the solution of the two-dimensional flow equations.

The parameter z_0 is the roughness length and is the distance above the bed at which the velocity is zero. Physically, it represents the deviation of the bed surface from the local average bed surface and typically is considered to be proportional to the dimensions of obstacles on the bed, such as bedform height or the diameter of gravel clasts. In the flow model, z_0 is related to the deviation of the bed surface on the computational grid from surveyed values. If the slope of the water surface were known, the constant of proportionality between z_0 and some measure of the deviation of the bed surface from local surveyed values, such as the standard deviation (σ_s), could be calculated from the average shear stress in the reach. Water-surface slope was not measured in the study reaches, however, so the constant of proportionality, typically taken to be 0.1, relating z_0 to the roughness length of gravel was used to relate the z_0 to σ_s . This leads to a z_0 of 20 cm. This extraordinarily high value of z_0 is a result of the extreme irregularities of the channel bottom that cannot be resolved by the computational grid. The ambient slope, S , for each reach was estimated from the channel roughness described above, the discharge at a known water-surface elevation, and the inlet channel shape. The slope was adjusted until the calculated discharge matched the known discharge.

The eddy viscosity, ε , is defined as:

$$\varepsilon(z) = u_* \kappa z \left(1 - \frac{z}{h}\right) \quad (10)$$

and is vertically-averaged for use in (2) and (3):

$$\varepsilon = \frac{u_* \kappa h}{6} \quad (11)$$

The assumption that the pressure field is hydrostatic, that is, the pressure is proportional to the distance below the river surface, is violated in some locations, such as where the flow is directed toward ledges and bedrock walls or where it enters and exits pools at the downstream ends of rapids. When a fluid is homogeneous in density and pressure is hydrostatic, the horizontal pressure gradient is independent of depth. In regions with ledges and pools, substantial vertical velocity components, hence nonhydrostatic pressure gradients, may be produced by accelerations or decelerations that vary with depth as a consequence of the obstructions and topographic contractions or expansions. Variation of the near-bottom pressure gradient relative to the depth-averaged value causes enhancement or reduction in the local boundary shear stress and a consequent response in the suspended-sand transport field. These effects, however, are local and primarily affect local rates of erosion or deposition, not the ultimate depositional pattern. Moreover, once substantial sediment deposition has occurred, many of the irregularities of the channel bed that produced the nonhydrostatic pressure field are removed, and the flow as well as the sand deposit adjust so that they are well represented by the model. The areas of interest in this bed-evolution model are the alluvial sections of the channel, in which the flow ultimately will satisfy the hydrostatic approximation. Where the flow remains nonhydrostatic, almost all of the sediment in suspension is passed through to the alluvial sections, and the details of how that is accomplished are not crucial for an accurate model.

Sediment-transport field. Sand transport is primarily in suspension in the Colorado River in the Grand Canyon because of the small grain size and high shear stresses. The average sand diameter measured by Schmidt and Graf [1990] in the reach between RM 62.5 and 75.6, which encompasses the study reach, is 0.13 mm, and that grain size was used in the calculations. The transport of suspended sand is governed by an advection-diffusion equation:

$$\frac{\partial c}{\partial t} + \frac{\partial cu}{\partial x} + \frac{\partial cv}{\partial y} + \frac{\partial cw}{\partial z} - \frac{\partial}{\partial x} \epsilon \frac{\partial c}{\partial x} - \frac{\partial}{\partial y} \epsilon \frac{\partial c}{\partial y} - \frac{\partial}{\partial z} \epsilon \frac{\partial c}{\partial z} + w_s \frac{\partial c}{\partial z} = 0 \quad (12)$$

where:

- c sediment concentration
- w_s sediment settling velocity
- w vertical fluid velocity

Equation (12) is solved for a given flow field with ten points in the vertical, concentrated near the water surface and near the bed. Equation (10) gives the eddy viscosity as a function of z, and the velocity as a function of z is supplied by (9).

The lower sediment-concentration boundary condition is calculated by first determining a reference concentration at $z = 0$. The reference concentration, c_a , determined from the relations of Smith and McLean [1977] is given by:

$$c_a = \frac{c_b \gamma s}{1 + \gamma s} \quad (13)$$

where c_b is the bed concentration and s is the normalized excess shear-stress:

$$s = \frac{\tau_{sf} - \tau_c}{\tau_c} \quad (14)$$

where the subscript sf indicates skin-friction shear stress, discussed in the section below, and τ_c is critical shear-stress for the initiation of significant particle motion [Shields, 1936]. The value of the constant γ has been updated to 0.004 by Wiberg [reported by McLean, 1992]. The distance above the bed corresponding to c_a , namely z_a , is at the top of the bedload layer and is determined from the expression presented by Dietrich [1982] with constants a_1 and a_2 as updated by Wiberg and Rubin [1985]:

$$z_a = d \frac{a_1 T_*}{1 + a_2 T_*} \quad (15)$$

where:

d grain diameter

$T_* = \tau_{sf}/\tau_c$

a_1 constant = 0.68

The coefficient a_2 is a function of grain size:

$$a_2 = 0.02035 (\ln(d))^2 + 0.02203 \ln(d) + 0.07090 \quad (16)$$

The lower sediment-concentration boundary condition at $z = z_0$ is calculated using the relation Rouse [1937] derived by neglecting the horizontal advection and diffusion terms in (12):

$$\frac{c}{c_a} = \left(\frac{z_a (h - z)}{z (h - z_a)} \right)^\phi \quad (17)$$

where ϕ is the Rouse number, defined as:

$$\phi = \frac{w_s}{\kappa U_{*sf}} \quad (18)$$

The boundary condition at the water surface is $c = 0$, consistent with (10).

Bed-evolution. The evolution of the bed over time is calculated from the sediment continuity equation:

$$\frac{\partial \eta}{\partial t} = -\frac{1}{c_b} \left(\frac{\partial q_s}{\partial x} + \frac{\partial q_s}{\partial y} \right) \quad (19)$$

where η is bed elevation and q_s is sediment discharge. Because the flow field adjusts rapidly to changes in the bed topography, the flow field is calculated as a series of steady flows conforming to the bed configuration. The finite-difference time step must be small enough to ensure a stable progression of the bed evolution over time. In the model, (19) is solved for the unsteady term over the entire grid, and then a time step is calculated such that the maximum change in bed elevation at any location is below a specified value, typically about one centimeter.

In many parts of the channel of the Colorado River in Grand Canyon, non-erodible materials are covered by only a veneer of sand or are exposed. A minimum bed elevation representing the surface of the bedrock and coarse gravel, therefore, must be specified. The bed topography measured before the Little Colorado River flood of January 1993 was used here as the minimum bed elevation. Although the Little Colorado River flood significantly increased the discharge in the main stem, the massive influx of sediment that came with the flood resulted in an event that was primarily depositional in the reaches close to the Little Colorado River mouth. Most of the measured cross sections discussed below showed no erosion. Minor amounts of erosion did occur at the downstream end of model reach 1 (Figure 1), and use of the pre-flood topography as a minimum bed elevation prevented the model from predicting the erosion in that area.

Application to the Little Colorado River Flood of January 1993

The cross sections established in 1992 are located in four of the first five pool reaches downstream from the Little Colorado River confluence, and each of these four reaches was modeled separately (Figure 1). The four modeled reaches are bounded upstream and downstream by constrictions or riffles through which the suspended sand passes with negligible deposition. The model was run at a constant discharge of $617 \text{ m}^3/\text{s}$ ($21,800 \text{ ft}^3/\text{s}$), which is the average discharge for the duration of the first and largest peak starting January 10 that lasted about six days (Figure 2).

The sediment-transport component of the model requires that the sediment flux into each model reach be specified as an upstream boundary condition. The sand discharge into each reach was set at $2.28 \text{ m}^3/\text{s}$, the average sand discharge in the Little Colorado River reported by Fisk during the period modeled [Gregory G. Fisk, USGS, personal communication]. This sand discharge yields a volume sand concentration of 0.37 percent, close to the 0.4 percent by volume that characterized the upper limit of sand concentration at this discharge prior to the closure of Glen Canyon Dam (David Topping, USGS, personal communication). In order to determine the fraction of the total shear-stress that was exerted as skin friction, equilibrium suspended-sand concentration fields were calculated for straight channels that had the cross-sectional shapes of the reach entrances, and the skin friction fraction was set such that the total sediment discharge matched the upstream sediment discharge boundary condition. Cross-stream advection and diffusion would have been sufficient during the flood in the 1 km reach between the mouth of the Little Colorado River and the first modeled reach to justify the assumption that sand was evenly distributed over most of the channel floor in this upstream zone and was moving downstream as it would in an alluvial channel. Moreover, the volume of suspended sand brought into the Colorado River by the flood was sufficient to warrant the application of this assumption to each of the subsequent reaches.

The model was run for simulated periods of six days. Changes in bed shape were rapid initially but were reduced over time as the bed approached a stable configuration, and six days was found to be sufficient to achieve a stable channel shape in all reaches.

Comparison of Measured and Computed Changes at Monumented Cross Sections

Accuracy of model results was determined by comparison of model-computed changes to changes measured at the monumented cross sections. Field measurement of other model computed fields, such as the flow or sediment-transport, with sufficient accuracy to test model results was not feasible, and comparison of measured and predicted bed changes provides the best method for model evaluation and is also the most relevant to the issues of interest in this report. Discrepancies between the measured and calculated profiles can be a result of subsequent low-stage redistribution of the sand prior to sampling the measured sections after the flood, use of improper estimates of local bed roughness, use of incorrect estimates of the locations of the gravel surface, and small spatial phase shifts in the computed fields because of the way topography was input to the model, as well as direct model error arising from oversimplification of the flow and sediment transport equations.

As mentioned above, the modeled pool reaches are separated by riffles formed where the channel is constricted and gravel and boulders are present because of debris fans at mouths of small, steep tributaries. Reach 1, including sections A1-A5, covers the first pool downstream from the Little Colorado River mouth (Figure 1). The left-bank debris fan deflects the thalweg toward the right bank at the upstream end of the reach, and at A1, the preflood topography showed a deep channel along the right bank at the upper end of a channel expansion and zone of recirculating flow along the left-bank downstream from the debris fan. Section A2 crosses the zone of recirculating flow in the expansion, and A3 is at the downstream end of the expansion (Figure 1). Sections A4 and A5 are in a region of relatively shallow flow upstream from the debris fan and riffle that form the downstream boundary of the reach. Section A1 aggraded over the entire section between the initial measurement in June 1992 and the post-flood measurement of January 1993. Aggradation was greatest, about 12 m, in the thalweg. Sections A2 and A3 aggraded as a result of the flood, but aggraded less than the upstream section. Sections A4 and A5 have shown little change over the entire measurement period [Graf et al., 1995b], suggesting that the bed is gravel or bedrock and this is not an area of temporary sand storage. The model predicts well the aggradation in the recirculation zone along the left bank, but underestimates the aggradation in the middle to river left part of cross section A1 (Figure 3). This is probably a result of remobilization of the sand upstream after the flood and prior to the January measurements.

Figure 3. Measured and computed cross sections A1-A5 from before and after the Little Colorado River flood of January 1993 for study reach 1.

Sections A6 and A7, in the second pool reach downstream from the confluence (Figure 1) both aggraded over their entire width during the Little Colorado River flood (Figure 4). The right-bank debris fan at the upstream end of the reach deflects the thalweg toward the left bank and forms an expansion and recirculation zone along the right bank. At A6, aggradation was greatest, about 9 m, within the expansion. Aggradation was greatest in the thalweg at section A7, about 13 m, but considerable aggradation also was measured along the right bank, where the section crosses the downstream end of the zone of recirculating flow. The model predicts less thalweg deposition and slightly thicker channel margin deposits in sections A6 and A7 than was measured, but the general shape and amount of deposition are well described by the model (Figure 4).

Figure 4. Measured and computed cross sections A6 and A7 from before and after the Little Colorado River flood of January 1993 for study reach 2.

Reaches 3 and 4, including sections B2-B4 and C1-C5, respectively, are separated by a large, mid-channel gravel bar and left-bank debris fan (Figure 1). Reach 3 is in an expansion between a right-bank debris fan and the gravel bar. The debris fan deflects the flow toward the left bank upstream from section B2, and the thalweg shifts from the left to the right bank in the area covered by the three sections. The bar surface is higher than river stages produced by power-plant releases, and flow was diverted around both sides of the bar at all stages reached during the flood. Section B2 is at the upstream end of the expansion, upstream from a zone of recirculating flow along the left bank. Little change was measured along the left side as a result of the flood. Some aggradation was measured along the right side of the section. Maximum aggradation was about 2 m. Section B3 crosses a zone of recirculating flow along the left bank between a small debris fan and the gravel bar. About 1 m of aggradation was measured in the recirculation zone, and about 6 m of aggradation was measured along the right side of the channel, shifting the thalweg toward the left bank slightly. Section B4, just upstream from the gravel bar, showed relatively little change. The bed degraded slightly over the central part of the section and aggraded about 4 m along the right bank and slightly along the left bank. The model appears to overestimate deposition outside the main channel in reach 3, but reproduces the general shape and magnitude of the observed changes (Figure 5).

Figure 5. Measured and computed cross sections B2-B4 from before and after the Little Colorado River flood of January 1993 for study reach 3.

A left-bank debris fan deflects the flow toward the right bank at the upstream end of reach 4. The sections in the pool downstream from the fan showed a pattern of change similar to sections A1-A5—the three upstream sections cross a large left-bank zone of recirculating flow and aggraded significantly over their entire lengths and the two sections downstream are in an area of shallower, more even flow and showed little change. Aggradation was by filling in of the left-bank eddy and the thalweg at section C1. Section C2 crosses a small right-bank eddy and the center of the larger left-bank recirculating zone, and infilling of both recirculation zones and the thalweg was measured. Maximum aggradation was about 12 m at sections C1 and C2 and about 6 m at section C3. Sections C4 and C5 are downstream from the zone of recirculating flow and show relatively little change as a result of the Little Colorado River flood. Reach 4 showed the greatest amount of aggradation and the best agreement between measured and computed cross-section changes (Figure 6).

On average, the model results agree well with measured changes in cross sections (Figures 3-6). The difference between the sums of the measured and computed cross-section areas is 5.6 percent. The percentage difference at cross sections can be quite large where little deposition occurred (sections C4 and A5, for example), but the overall error is small because these cross sections contribute little to the total deposition, and because percentage difference between cross sections where deposition is large (C1-C3) tends to be small, and the errors tend to cancel.

Figure 6. Measured and computed cross sections C1-C5 from before and after the Little Colorado River flood of January 1993 for study reach 4.

Comparison of Preflood and Postflood Topography in the Four Study Reaches

Sediment was transported from the mouth of the Little Colorado River to the first riffle downstream and was deposited on the channel bottom in reach 1, filling in the thalweg and creating a sand bar in the region of lowest shear stress in the left-bank expansion (Figure 7). Aggradation was computed by the model over much of the area of the reach, but little channel change was produced in the area of flow convergence downstream from 200 m below the entrance of the model reach, in agreement with measurements cross sections at A4 and A5. In reach 2, a bar was built within the recirculation zone along the right bank at the upstream end of the reach, the thalweg in the upstream part of the reach was filled in, and little change was predicted by the model for the downstream half of the reach (Figure 8). A similar pattern of deposition in the thalweg and along the banks in channel expansions downstream from debris fans is shown by model results for reach 3 (Figure 9) and reach 4 (Figure 10).

Computed Depositional Volumes and Rates of Sand Accumulation

The volume of the deposit was calculated by integrating the difference between the preflood and postflood bed elevations over the grid area. The computed depositional volumes were 3.4×10^4 , 4.5×10^4 , 5.0×10^4 , and 23×10^4 m³ for reaches 1-4, respectively. Computed volumes are about 15 percent of estimated sand influx during the 15 day duration of the Little Colorado River high discharge.

Figure 7. Initial topography and flow field in model reach 1 (left) and the topography and flow field after 6 days (right).

Figure 8. Initial topography and flow field in model reach 2 (left) and the topography and flow field after 6 days (right).

Figure 9. Initial topography and flow field in model reach 3 (left) and the topography and flow field after 6 days (right).

Figure 10. Initial topography and flow field in model reach 4 (left) and the topography and flow field after 6 days (right).

If pools downstream from the modeled reaches stored the same volume of sand as the modeled reaches, then all sand delivered to the Colorado River by the January 1993 Little Colorado River flood would have been deposited initially in the first 20 km downstream from the confluence. Available data on channel geometry show that the river just downstream from the modeled reaches is wider than the modeled reaches. Flow widths at a discharge of $141 \text{ m}^3/\text{s}$ in the 2.9-km modeled reach average about 89 m whereas those in the 20 km downstream average about 98 m [computed from data of Smith and Furey, 1995]. Given the far greater capacity for sand storage in reach 4, which is a function at least in part of its greater width, it is likely that the reach extending 20 km downstream from the study reach has, on average, a sand storage capacity at least as large as the average of the study reaches. Significant deposition was observed after the Little Colorado River flood that extended far below the confluence. A layer of sediment deposited on sand bars as far as 180 km downstream from the Little Colorado River mouth was observed by the authors and by other workers that visited the area after the flood [G.G. Fisk, S.M.D. Jansen, USGS, personal communication]. These deposits must have been formed from a combination of sand that was resuspended locally from the channel bed and banks and silt-sized sediment that also was derived locally or carried long distances by the higher discharges caused by the flood.

Each of the modeled reaches accumulated sand at a rapid rate initially, but the rate of accumulation became negligible as the reaches approached their capacity (Figure 11). This change in rate is most striking in reach 3, which filled in about one day as a result of its relatively small eddy zones and short length. The lower capacity reaches, 1 and 2, also filled at lower rates, taking about two days to fill. Reach 4, which had the largest capacity, continued to accumulate significant amounts of sand for about three days. The first three reaches accumulated sand at smoothly decreasing rates, but in reach 4, the volume of deposited sand fluctuated slightly after initial filling as a result of the growth and downstream transport of bars in the main channel.

The fraction of the initial channel volume occupied by the deposited sand varied between 8 percent, in reach 1, and 47 percent, in reach 4 (Figure 11). The smallest volume fraction was in reach 1, which also had the smallest total volume of sand, and the highest fraction is in reach 4, which also had the largest volume deposited.

With a high influx of sediment, the reach-integrated deposition rates are very high initially and fall off rapidly as the channel asymptotically approaches its capacity at the prescribed stage (Figure 11). As the channels become less effective as sediment traps, they become more effective as sediment conduits. In reach 3, nearly all of the sand introduced at the upstream boundary was passed to the next reach after one day, and in reach 4, which stored the most sand, it took only 2-3 days.

Figure 11. Relation of sand volume computed by the model to time (top) and sand volume normalized by flow volume (bottom) for each of the four study reaches.

Deposition rates also varied within reaches by the three depositional environment defined above: main channel, eddy-associated, and channel margin. A simple algorithm based on the flow field calculated with the initial topography was used to delineate these depositional environments. The results are consistent with field observation and provide a means for computing the sand storage within depositional environments. The main channel is distinguished from eddy-associated and channel margin by flow velocity. A flow velocity of 0.45 m/s used to distinguish between main channel and deposits outside the main channel gave good results. The eddy-associated and margin deposits are further distinguished by flow direction: near-bank upstream flow is clearly within an eddy, and the transition from eddy-associated deposit to channel margin deposit was defined as the location where the near-bank downstream flow vectors are nearly parallel to the bank.

The depositional environments (Figure 12) and the differences in deposition rates by environment (Figure 13) are well represented in reach 4. This reach is wide and has an expansion ratio of about 3, close to the average value of 2.9 [Schmidt and Graf, 1990] and the value for reach 3, but significantly higher than those for reaches 1 and 2, which have expansion ratios of about 1.7. The width and expansion ratio in reach 4 are conducive to large, well-formed eddies. As a result, about 1/3 of the large volume of sand deposited in reach 4 formed eddy-associated deposits. The main channel, which had a deep depression just downstream of the pool inlet, accumulated about 63 percent of the total sand deposited in reach 4. The rates of deposition in the two environments, however, are different, with the main channel filling much more rapidly.

Figure 12. Initial topography of model reach 4 with area defined as main channel, recirculation zones, and channel margins.

Figure 13. Change in sediment volume (top) and rate of change of sediment volume (bottom) with time for the total area of model reach 4 and for areas defined as main channel, recirculation zones, and channel margins.

Discussion

The distribution of the sand deposits from the Little Colorado River floods of January, 1993, indicate that channel morphology is at least as important as reach planimetric area in determining the volume of sand stored. The surface area of reach 1 is about 93 percent that of reach 4, but stored only about a seventh of the sand volume. The longer, relatively narrow morphology of reach 1 contributed to its ineffectiveness as a sediment trap. Only in the depression just downstream of the inlet, in the expansion on the left side of the channel near the inlet, and in a narrow strip along the right bank were significant amounts of sand deposited in that reach. The downstream part of reach 1 is an area of flow convergence due to the relatively shallow depths and would have eroded under normal dam releases if the channel were entirely alluvial. Measurements at cross section A3 (Figure 3) show some erosion along the right half of the channel during the high flows, possibly due to a breach of a gravel lag by the high bed stresses induced by the flood flows combined with an influx of sand that filled the interstices of the gravel bed. The downstream part of reach 1 is likely to remain inactive because bed stresses are sufficient to pass sediment through without deposition even under normal dam operation. Reach 4, on the other hand, has a narrow entrance and exit with wide embayments on both sides as well as a deep hole just downstream from the entrance. Flow expansions in these areas lead to large deposits along the channel margins and within the main channel. Reaches 2 and 3 each cover a smaller area than reaches 1 and 4, and are between reaches 1 and 4 in their effectiveness as sand traps. The volume of sand deposited in reaches 2 and 3 is greater than that in reach 1, although the volumes of reaches 2 and 3 are smaller than that of reach 1.

Whereas reaches 1, 3, and 4 accumulated sand mostly in the main channel with only 5, 4, and 33 percent of the total, respectively, depositing in the eddy zones, 67 percent was deposited in the eddy zone in reach 2. Reach 2 differs from the other three reaches in that the main channel depression is bordered on the left bank by a nearly vertical bedrock wall that confines the main flow in a high velocity, high shear-stress zone. The calculated shear stresses in that zone are sufficient to keep the depression swept clear of sand. Measurements at cross section A7 show more sand in the depression than calculated by the model. This is probably a result of redistribution of sand at lower discharges following the Little Colorado River flood. The assumption of hydrostatic flow built in to the model may degrade the accuracy of the model in the region adjacent to the bedrock wall, but the turbulent, nonhydrostatic flow in nature would tend to enhance the suspension of sand in opposition to deposition rather than in its favor.

Depositional patterns in the study reaches are an expression of the shear-stress divergences induced by the channel morphology. The sensitivity of sediment transport to the flow field can be illustrated with the simple relation proposed by Engelund and Hanson [1967] in which the transport of suspended sediment is proportional to the boundary shear-stress to the 5/2 power. If the local boundary shear-stress is formulated as a function of the velocity, as is the case in the flow model, it is primarily a function of U^2 and depends only weakly on the depth in Equations (5) and (8). As a result, the sediment discharge is proportional to U^5 . The irregularity of the channel shape and the accompanying reductions in velocity where the flow enters the expansions lead to deposition if the sediment supply is sufficient and, in the case of margin deposits, the stage is sufficiently high. Large negative shear-stress divergences exist in vertical and lateral channel expansions which function as effective sediment traps.

The combination of large negative shear-stress divergences and high sediment concentrations just downstream from the constrictions at the upper ends of the modeled pools causes the depressions in those areas to fill rapidly (Figure 13). The magnitude of the negative shear-stress divergences is reduced as the holes fill, resulting in a reduction in the rate of deposition. Similarly, the magnitude of the negative shear-stress divergences in the lateral expansions near the eddy zones and along the channel margins is reduced as sand is deposited in those regions, thereby reducing flow expansion and confining most of the flow within the newly self-formed main channel. Deposition forms a new shape over time that is in equilibrium with the sediment influx. When that point is reached, the main channel becomes a sediment conduit rather than a sediment trap, and the full sediment load is delivered to the head of the next pool. This process is well-illustrated by results of computations for reach 4. The rate of deposition in the channel starts high but drops rapidly (Figure 13). The rate of deposition in the eddies starts at a lower rate, increases slightly as a result of enhanced sediment discharge into the eddy zones as the main channel fills, and then decreases on average over the remainder of the event.

Deposition of sand can have a strong affect on the flow field over time. The wide lateral expansions and deep main channel initially contribute to the formation of large recirculation zones on both sides of the main channel in reach 4 (Figure 14a). Filling of the main channel and deposition along the channel margins extending downstream from the inlet causes the thalweg zone to narrow and become shallower, and causes the high-velocity main-channel flow to impinge on the recirculation zones (Figure 14b,c). In the eddy zones, deposition is favored along the right bank for the first 2 days (Figure 14d,e), followed by increased deposition on the large bar along the left bank (Figure 14f). Establishment of the left-bank bar deflects flow back towards the right bank, causing the right-bank deposits to be eroded. Some of the sand excavated from the right bank temporarily formed a mid-channel bar (Figure 14g) that migrated down the main channel. At the end of six days, a stable shape formed with a large bar along the left bank and the main flow occupying the right half of the channel (Figure 14h). The dynamic interplay between the left and right bank deposits was unique to reach 4. In the other three reaches, sand accumulated continuously at a decreasing rate in the depositional sites.

Figure 14. Initial channel morphology and flow pattern for model reach 4 (A) and the morphology and flow pattern 6 hours (B), 12 hours (C), 24 hours (D), 2 days (E), 3 days (F), 4 days (G), and 6 days (H) after the beginning of model simulation.

The complexity of the calculated depositional history in reach 4 suggests that in addition to pool topography being too complicated spatially to be resolved adequately with only a few measured cross sections and a simple interpolation scheme, the evolving deposit could not be accurately represented by a small number of cross sections measured once or a few times during the 6 day period. The potential for this style of bed evolution is particularly great in the broad reaches that form the most effective sediment traps, because the breadth of such reaches permits a complicated interaction between the flow and evolving bed topography that allows the formation of complex, ephemeral bar forms.

The finding that recirculation-zone deposition rates are lower than deposition rates in the main channel in three of the four study reaches, especially during the early stages of a high-concentration sediment influx when the main channel is filling, is consistent with observations of Schmidt [1987]. He found that a very small percentage (less than 1.5 percent) of the estimated sand influx from a Paria River flood was deposited in recirculation zones in the 2.4 km just downstream from the confluence. The Paria River flood occurred when the Colorado River was near its peak daily discharge, estimated by Schmidt to be about 460 m³/s, and lasted only about 7 hours. The Paria River discharges were above 28 m³/s for only 3 hours. The short duration of the Paria River flood prevented deposition from developing beyond the early stage in which the main channel is far more effective in trapping sediment, and recirculation-zone deposition was therefore not significant.

The greatest benefit for sand-dependent riparian environments from the limited sediment supply is achieved by maximizing the volume of sand deposited along the channel margins and minimizing the volume of sand transported downstream. Sand deposited at high discharges along the channel margins above river stages corresponding to low discharges during normal dam operation is gradually fed back into the main channel by wind, foot traffic on camping beaches, by undermining and collapse of sand bars, and through sapping induced by fluctuating flows. Although storage of sand on the channel margins is temporary, these deposits are relatively stable compared to the ones in the channel. Channel deposits are especially significant in reach 4, which is by far the most effective sediment trap of the four study reaches (Figure 11). The capacity of reach 4 to trap such large volumes of sediment in the main channel during a large sediment influx is evidence that it is equally ineffective at retaining sediment during normal flows. After tributary flooding ceases and sediment-free water is flowing over the channel deposits, the sand is evacuated from the storage sites in main-channel depressions and carried downstream. This process becomes particularly effective when discharges surpass 425 m³/s (15,000 ft³/s), which is about where suspended-sand transport becomes significant [Smith and Wiele, 1995].

Recommendations for future operation of Glen Canyon Dam have included occasional discharges exceeding power-plant capacity to move sand from the channel bottom and deposit it along the channel flanks [BOR, 1994]. The frequency and duration of releases best suited to this end will require a careful balance between sand supply and discharge. Releases that are too high, too long, or too frequent will deplete the sand stored in the channel, result in the transport of excessive amounts of sand into Lake Mead, 346 km downstream, and possibly cause erosion of deposits initially formed by the high flow. On the other hand, sand in the channel is continuously transported downstream at rates determined by water discharge and sand coverage of the bed and will be lost to Lake Mead anyway if the high releases are too infrequent. If sand is to be retained in the part of the canyon upstream from the confluence with the Little Colorado River, then it is important that the sand be transported to the flanks of the channel before the flood-produced main-channel sand deposit are washed downstream.

Summary and Conclusions

Survival of a healthy riparian zone along the Colorado River in the Grand Canyon depends upon wise management of a severely limited sediment supply. The riparian environment depends not only on the volume of sediment available, but also on its placement. Simple sediment accounting methods based on sediment rating-curves developed for a few sites in the 386 km river corridor lack the accuracy and resolution to determine sediment budgets in critical reaches, especially over short time periods (months to years) and provide no information about depositional or erosional sites. As a result, ecologically sensitive management requires pool-scale monitoring and evaluation of processes and sand-dependent resources.

The volumes of sand stored in four pools downstream from the confluence and the processes that determine the distribution of sand among the primary pool-scale depositional sites, eddy-associated, channel margin, and main channel deposits, were evaluated in this study with a combination of field measurements and modeling. The field measurements were limited to reduce logistical costs of the study and to minimize the impact on Grand Canyon National Park and associated sensitive environments. These field data consisted of cross sections measured with sufficient accuracy to determine changes in local channel shape and cross-section area as a result of deposition and erosion and of bathymetric surveys from which gridded topography for use in the models could be constructed. The model computes flow fields, sediment-transport fields, and bed evolution and is used to interpolate, both in time and space, between the cross-section measurements.

The Little Colorado River flood of January 1993, supplied the Colorado River with about 4.17 Tg of sand. Fifteen percent was deposited in the first 3 km below the confluence and most of it was deposited within 20 km or so of the source. Flood deposits along the channel margins and within and around recirculation zones farther downstream were a consequence of the elevated stage, and sand in these deposits came primarily from sand that had been stored within the main channel.

Deposition rates and volumes of sand stored are quite variable among pools and depositional environments. Both the rate and volume stored in pools depend on pool morphology. The pool in this study that is wide and has a large expansion ratio, reach 4, accumulated four to seven times as much sand as each of the other three reaches. Deposition in reaches 2 and 3 was limited by their relatively short length and in reach 1 by its long narrow shape. All of the reaches accumulated sand rapidly initially and reached their storage capacity within 3 days. After that, all of the sand delivered to the pools was passed through to the next pool downstream. Depressions that are characteristically located in the main channel just downstream from the pool inlet accumulate sand at a rapid rate with an influx of sediment-laden water. Deposition in these depressions causes the main channel to tend towards a shape that is in equilibrium with the sediment transport. The deposition rate in the depressions, as a result, is highest initially and drops to zero if the sediment influx is of sufficient intensity and duration, as it was during the Little Colorado River floods of January, 1993. The time required for the channel to reach equilibrium with the sediment transport was about one to three days. Deposition rates along the channel flanks were much lower than in the main channel in the 4 study reaches, and the main channels accumulated about twice the total volume of sand than was deposited along the channel flanks.

Dam releases designed to replenish the sand that supports the native riparian environments using main-channel sand will be most effective when the main channel deposits are full from recent tributary flooding. The main-channel deposits begin eroding as soon as tributaries cease supplying sediment. The long-term stability of eddy-associated deposits and deposits along the channel margins is enhanced by their location above the waterline generated by typical power-plant flows. They are still vulnerable, however, to erosion by several processes, but at a far slower rate than in the main channel.

Acknowledgments

Funding was provided by the Bureau of Reclamation as part of Glen Canyon Environmental Studies.

References

- Akima, H., A method of bivariate interpolation and smooth surface fitting for irregularly distributed data points, *ACM Trans. Math. Software*, 4, 148-159, 1978.
- Andrews, E.D. and J.M. Nelson, Topographic response of a bar in the Green River, Utah to variations in discharge, In: Ikeda, S. and Parker, G. (eds.), *River Meandering*, 1989.
- Bennett, J.P., Sediment transport simulations for two reaches of the Colorado River, Grand Canyon, Arizona, *Water Resources Investigations Report 93-4034*, U.S. Geol. Surv., 1993.
- Bureau of Reclamation, Operation of Glen Canyon Dam: Colorado River Storage Project, Arizona, Final Environmental Impact Statement, December, various paging, 1994.
- Chow, V.T., Maidment, D.R., and Mays, L.W., *Applied Hydrology*, McGraw-Hill, New York, 1988.
- Dietrich, W.E. Flow, boundary shear stress, and sediment transport in a river meander. Unpublished Ph.D. dissertation, University of Washington, Seattle, Washington, 1982.
- Dolan R., A.D. Howard, and D. Trimble, Structural control of rapids and pools of the Colorado River in the Grand Canyon, *Science*, v.202, 629-631, 1978.
- Engelund, F. and F. Hanson, A monograph on sediment transport in alluvial streams, in *Teknisk Verlag: Copenhagen, Denmark*, Technical University of Denmark, 63 pp., 1967.
- Environmental Systems Research Institute, Inc., *ARC/INFO User's Guide—Surface Modeling with TIN™*: Environmental Systems Research Institute, Inc., Redlands, CA, various pagings, 1991.
- Graf, J.B., S.M.D. Jansen, G.G. Fisk, and J.E. Marlow, Bathymetry and topography of the Colorado River, Little Colorado River to Tanner Rapids, *Open-File Report 95-###*, U.S. Geol. Surv., 7 plates, 1995a
- Graf, J.B., J.E. Marlow, G.G. Fisk, and S.M.D. Jansen, Sand storage changes in the Colorado River downstream from the Paria and Little Colorado Rivers, June 1992 to February 1994, *Open-File Report 95-##*, U.S. Geol. Surv., ## p., 1995b.
- Howard, R.E. and R. Dolan, Geomorphology of the Colorado River in the Grand Canyon, *Journal of Geology*, 89(3), 269-298, 1981.
- Jansen, S.M.D., J.B. Graf, J.E. Marlow, and G.G. Fisk, Monitoring channel sand storage in the Colorado River in Grand Canyon, *Fact Sheet FS-120-95*, U.S. Geol. Surv., 1 p., 1995.
- Kieffer, S.W., The rapids and waves of the Colorado River, Grand Canyon, Arizona, *Open-File Report 87-096*, U.S. Geol. Surv., 1987.
- Keulegan, G.H., Laws of turbulent flow in open channels, *Res. Paper RP1151*, National Bureau of Standards, 21, 707-741, 1938.

- Lighthill, M.J., and Whitham, G.B., On kinematic waves, I: flood movement in long rivers. *Proc. R. Soc. London A*, 229, 1178, 1955.
- McCullagh, M.J. and C.G. Ross, Delaunay triangulation of a random data set for isarithmic mapping, *Cartographic J.*, 17, 93-99, 1980.
- McLean, S.R., On the calculation of suspended sediment load for noncohesive sediments. *J. Geophys. Res.* 97 (C4), pp. 5759-5770, 1992.
- Nelson, J.M. and J.D. Smith, Evolution and stability of erodible channel beds, In: Ikeda, S. and Parker, G. (eds.), *River Meandering*, 1989.
- Nelson, J.M., R. McDonald, and D. Rubin, Flow and sediment transport in lateral separation eddies, in review, 1995.
- Patankar, S.V., Numerical Heat Transfer and Fluid Flow. *Hemisphere*, Washington, D.C., 1980.
- Rouse, H., Modern conceptions of the mechanics of turbulence, *Trans. Am. Soc. Civil Engrs.*, 102, 1937.
- Rubin, D.M., J.C. Schmidt, and J.N. Moore, Origin, structure, and evolution of a reattachment bar, Colorado River, Grand Canyon, Arizona, *J. Sed. Pet.*, 60, 982-991, 1990.
- Schmidt, J.C., Geomorphology of alluvial-sand deposits, Colorado River, Grand Canyon National Park, Arizona. Unpublished Ph.D. dissertation, Johns Hopkins University, Baltimore, 1987.
- Schmidt, J.C. and J.B. Graf, Aggradation and degradation of alluvial sand deposits, 1965 to 1986, Colorado River, Grand Canyon National Park, Arizona, *Prof. Paper 1493*, U.S. Geol. Surv., 74 p., 1990.
- Shields, A, Application of similarity principles and turbulence research to bed-load movement, (in German), *Mitteil. Preuss. Versuchanst. Wasser, Erd, Schiffsbau*, Berlin, 26, 1936.
- Shimizu, Y. and T. Itakura, Practical computation of two-dimensional flow and bed deformation in alluvial streams. Civil Eng. Res. Inst. Report, Hokkaido Development Bureau, Sapporo, 1985.
- Shimizu, Y., I. Tadaoki, and H. Yamaguchi, Calculation of two-dimensional flow and bed deformation in rivers. Proc. XXII Cong. IAHR, Vol. A, pp. 201-206, 1987.
- Smith, J. Dungan. and S. R. McLean, Spatially averaged flow over a wavy surface, *J. Geophys. Res.*, 82, 12, 1735-1746, 1977.
- Smith, J.D., and P. Furey, Generation of channel topography for flood-wave routing, in preparation, 1995.
- Smith, J.D. and S.M. Wiele, Exchange of sand between the bed and margins of rivers with perimeters composed predominately of gravel and bedrock, *EOS*, 75:44, 1994.
- Smith, J. Dungan and S.M. Wiele, Flow and sediment transport in the Colorado River between Lake Powell and Lake Mead, in prep.
- Webb, R.H., P.T. Pringle, and G.R. Rink, Debris flows from tributaries of the Colorado River, Grand Canyon National Park, Arizona, *Prof. Paper 1492*, U.S. Geol. Surv., 39 p., 1989.

Werth, L.F., P.J. Wright, M. J. Pucherelli, D.L. Wegner, and D.N. Kimberling, Developing a geographic information system for resources monitoring on the Colorado River in the Grand Canyon, *Report Number R-93-20*, Dept. of the Interior, Bureau of Reclamation, Denver, Colorado, 46 p., 1993.

Wiberg, P.L. and D.M. Rubin, Bed roughness produced by saltating sediment, *J. Geophys. Res.*, 94, C4, 5011-5016., 1985.

Wiele, S.M., A computational investigation of bank erosion and mid-channel bar formation in gravel-bed rivers. Unpublished Ph.D. dissertation, University of Minnesota, Minneapolis, 1992.

Wiele, S.M. and Smith, J. Dungan, A reach-averaged model of diurnal discharge wave propagation down the Colorado River through the Grand Canyon, in review, 1995.

Wilson, R.T., Sonar patterns of Colorado River bed, Grand Canyon, *Proceedings of the Fourth Federal Interagency Sedimentation Conference*, 2, 5-133 to 5-142, Las Vegas, Nevada, 1986.

Figure 1. Location of model reaches, measured cross sections, and streamflow gaging stations used in the study.

2. Reconstructed instantaneous discharge at the mouth of the Little Colorado River and in the mainstem Colorado River downstream from the confluence during the flood of January 1993.
3. Measured and computed cross sections A1-A5 from before and after the Little Colorado River flood of January 1993 for study reach 1.
4. Measured and computed cross sections A6 and A7 from before and after the Little Colorado River flood of January 1993 for study reach 2.
5. Measured and computed cross sections B2-B4 from before and after the Little Colorado River flood of January 1993 for study reach 3.
6. Measured and computed cross sections C1-C5 from before and after the Little Colorado River flood of January 1993 for study reach 4.
7. Initial topography and flow field in model reach 1 (left) and the topography and flow field after 6 days (right).
8. Initial topography and flow field in model reach 2 (left) and the topography and flow field after 6 days (right).
9. Initial topography and flow field in model reach 3 (left) and the topography and flow field after 6 days (right).
10. Initial topography and flow field in model reach 4 (left) and the topography and flow field after 6 days (right).
11. Relation of sand volume computed by the model to time (top) and sand volume normalized by flow volume (bottom) for each of the four study reaches.
12. Initial topography of model reach 4 with area defined as main channel, recirculation zones, and channel margins.
13. Change in sediment volume (top) and rate of change of sediment volume (bottom) with time for the total area of model reach 4 and for areas defined as main channel, recirculation zones, and channel margins.
14. Initial channel morphology and flow pattern for model reach 4 (A) and the morphology and flow pattern 6 hours (B), 12 hours (C), 24 hours (D), 2 days (E), 3 days (F), 4 days (G), and 6 days (H) after the beginning of model simulation.

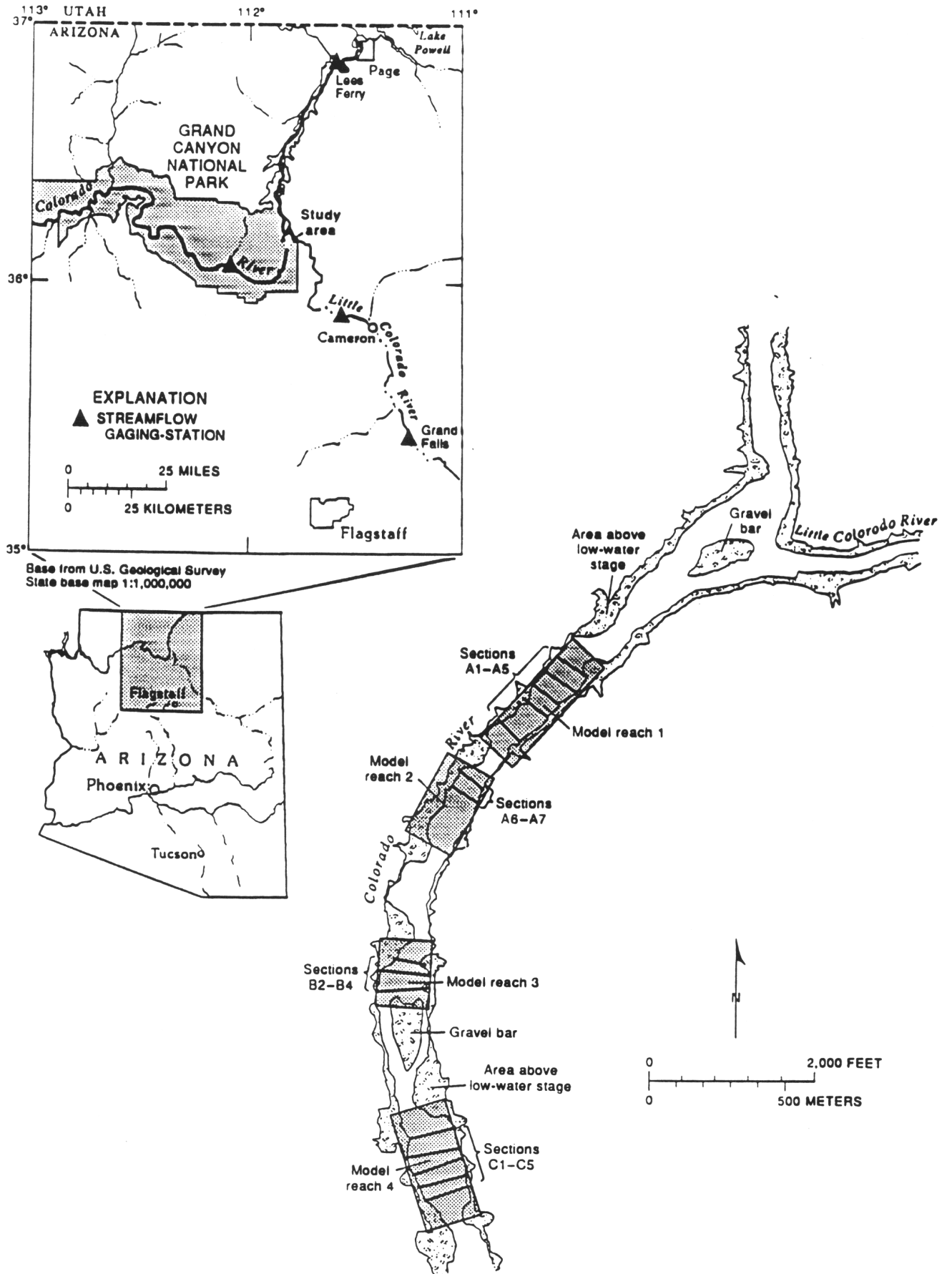
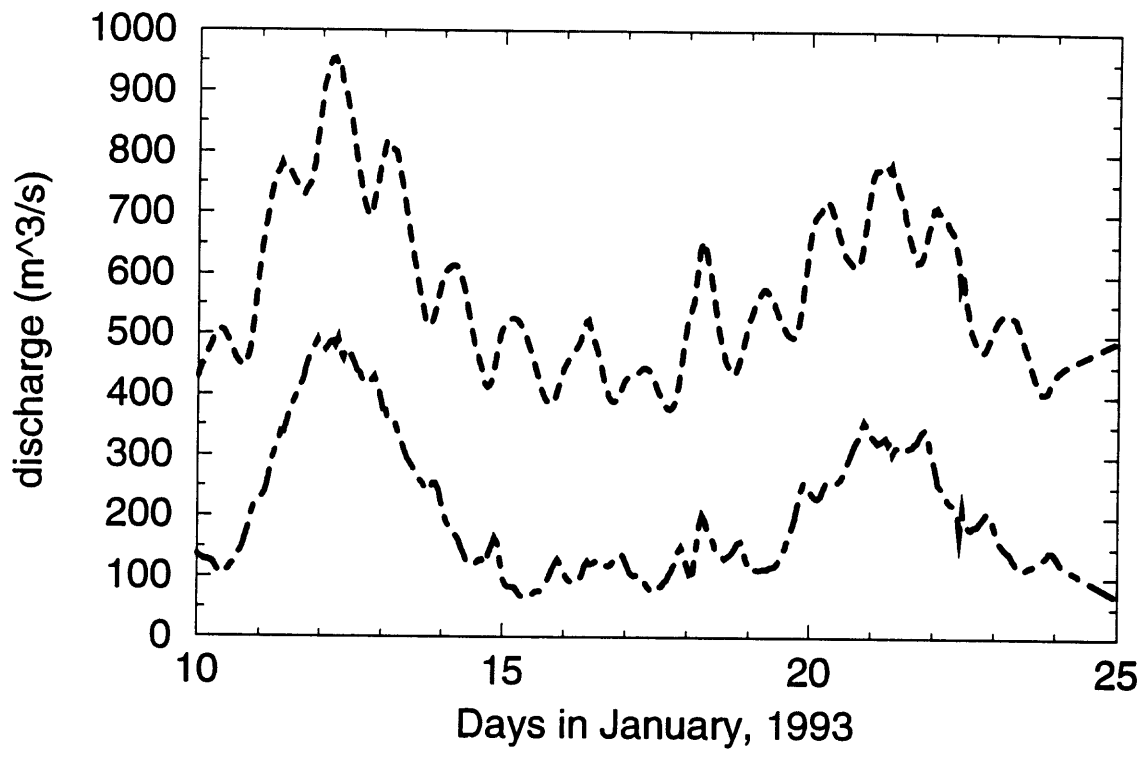


Figure 1. Location of model reaches, measured cross sections, and streamflow-gaging stations used in the study



----- mainstem discharge below the mouth of the LCR
----- LCR inflow into the mainstem

fig 2

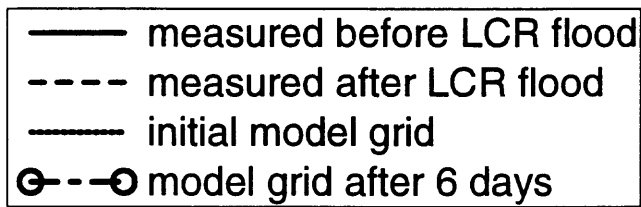
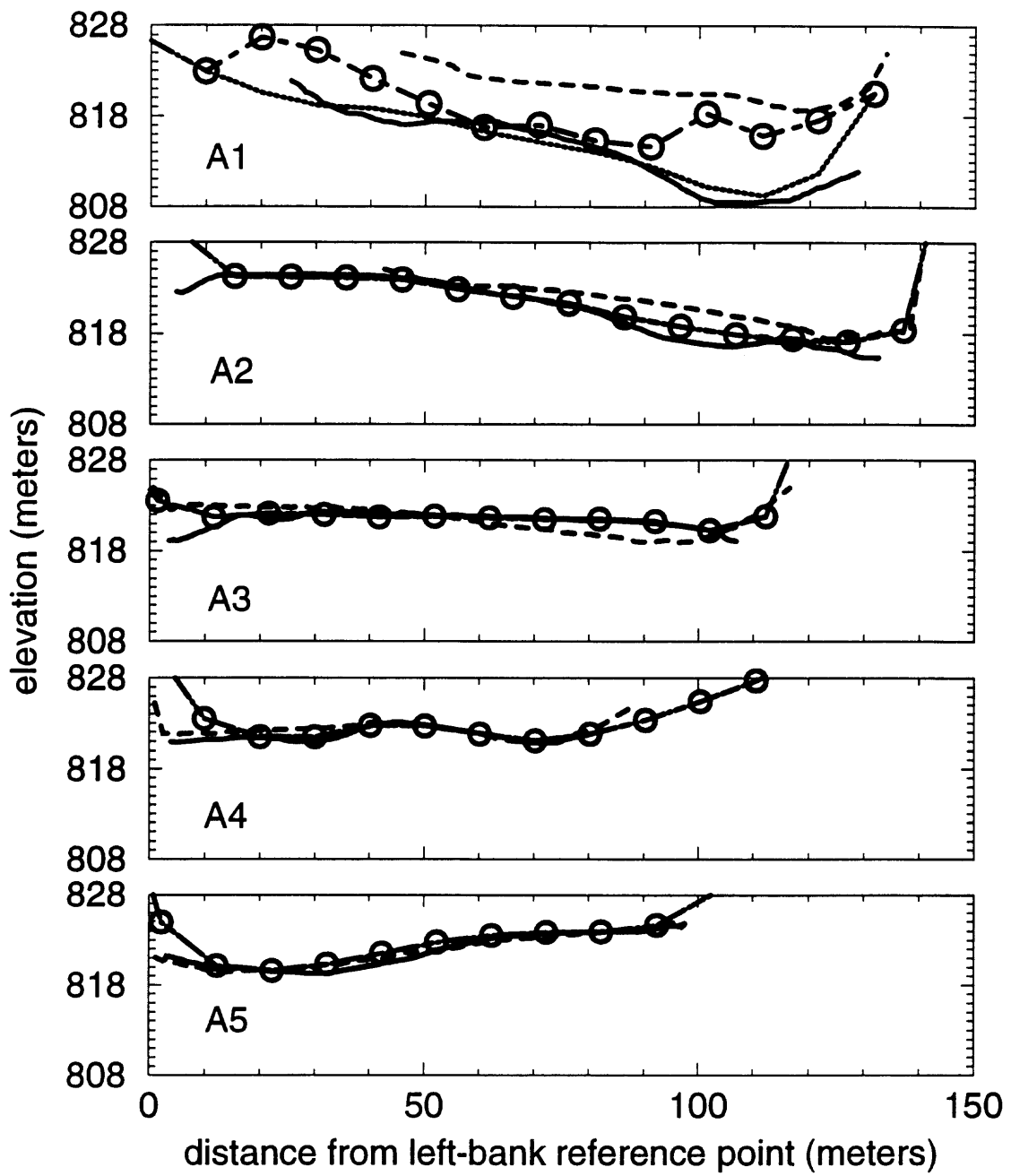


Fig 3

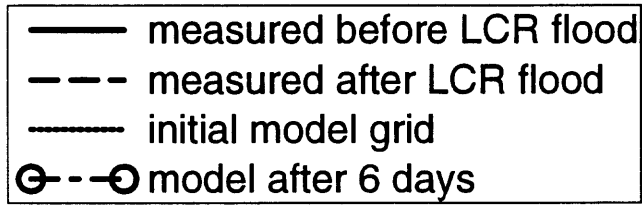
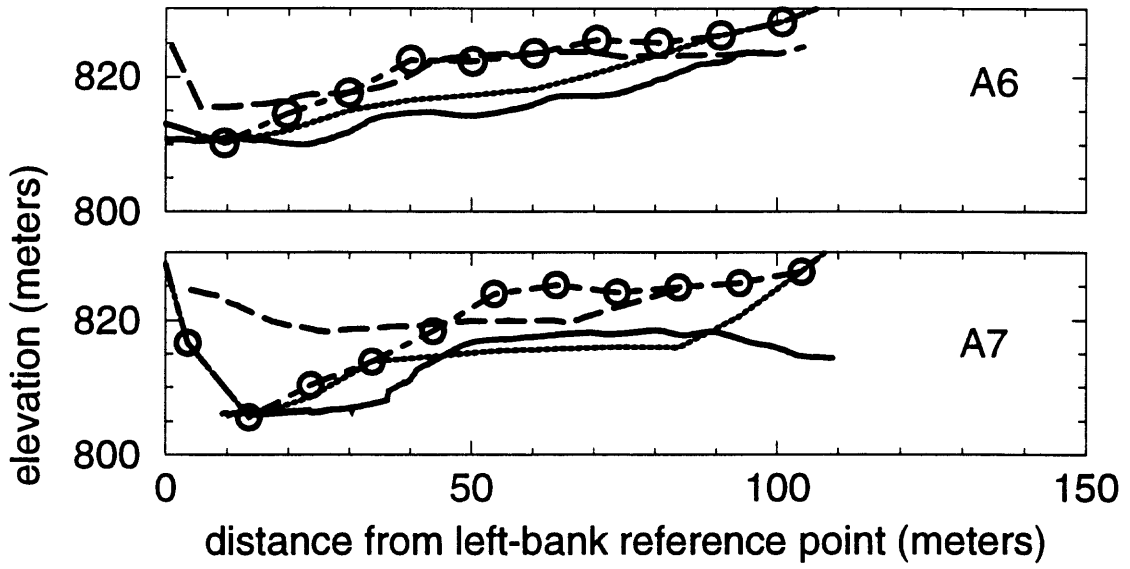


Fig 4

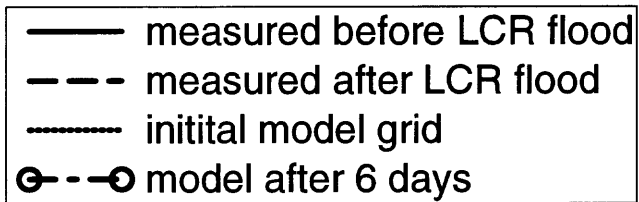
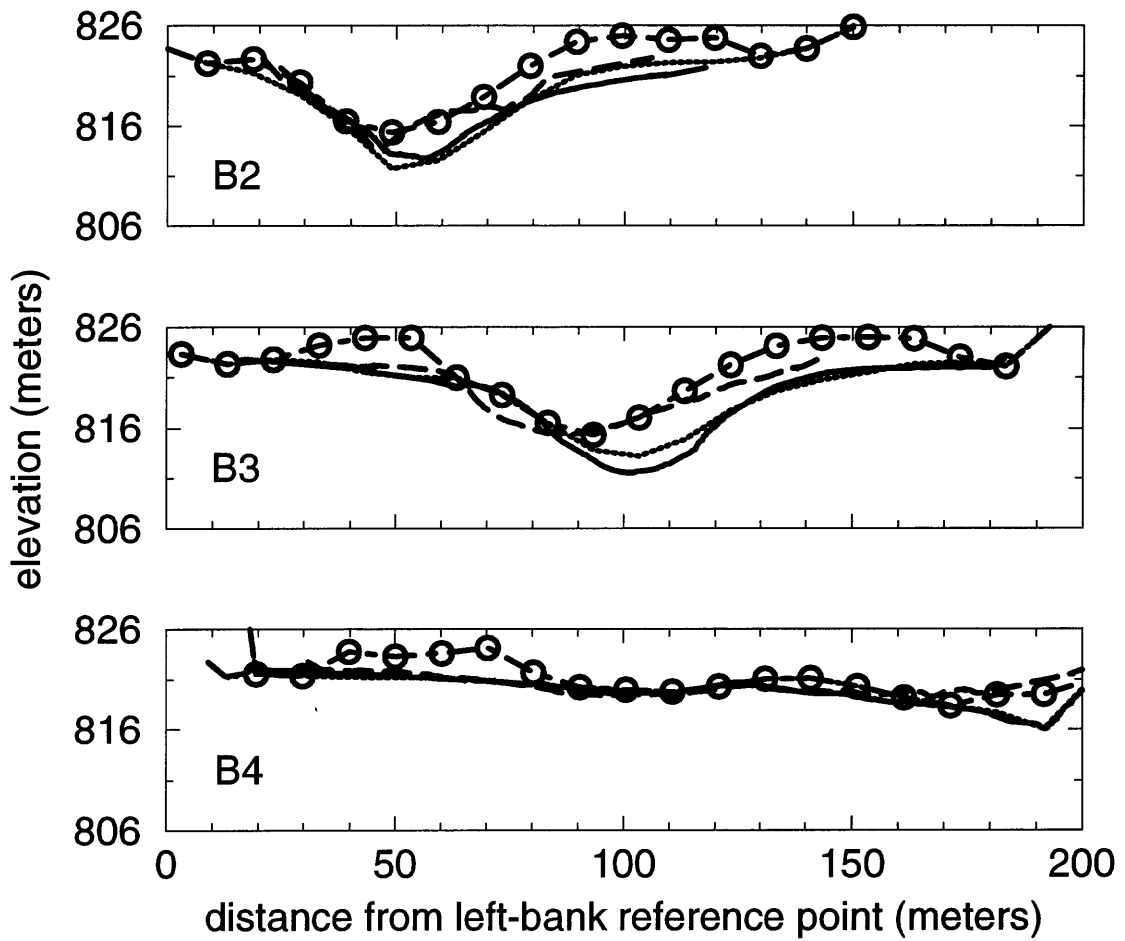


Fig 5

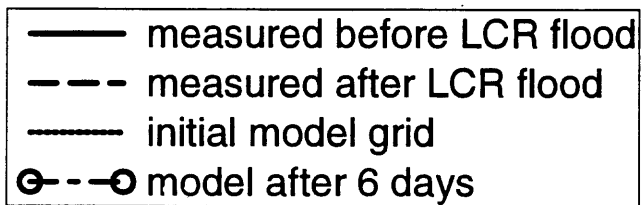
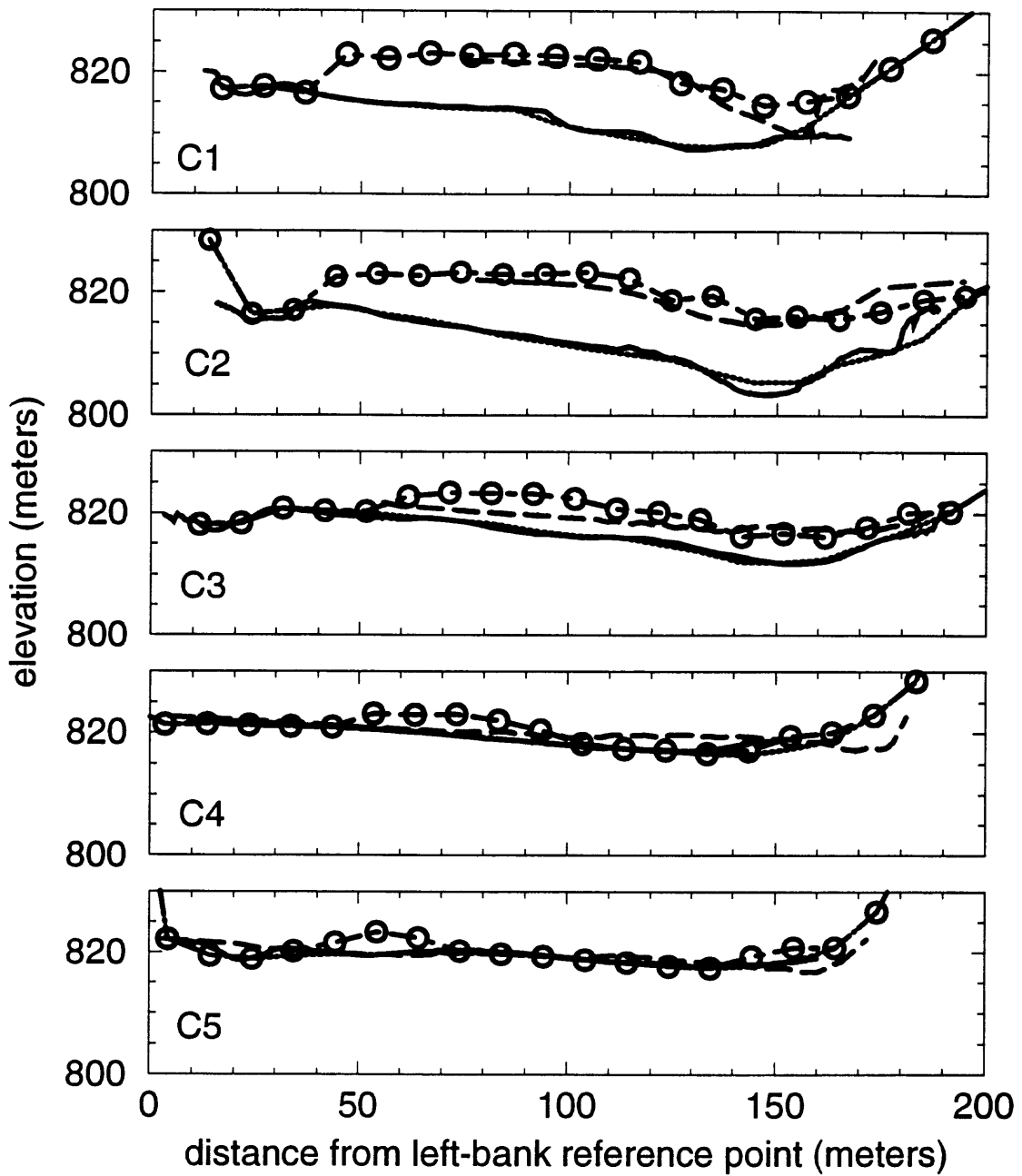
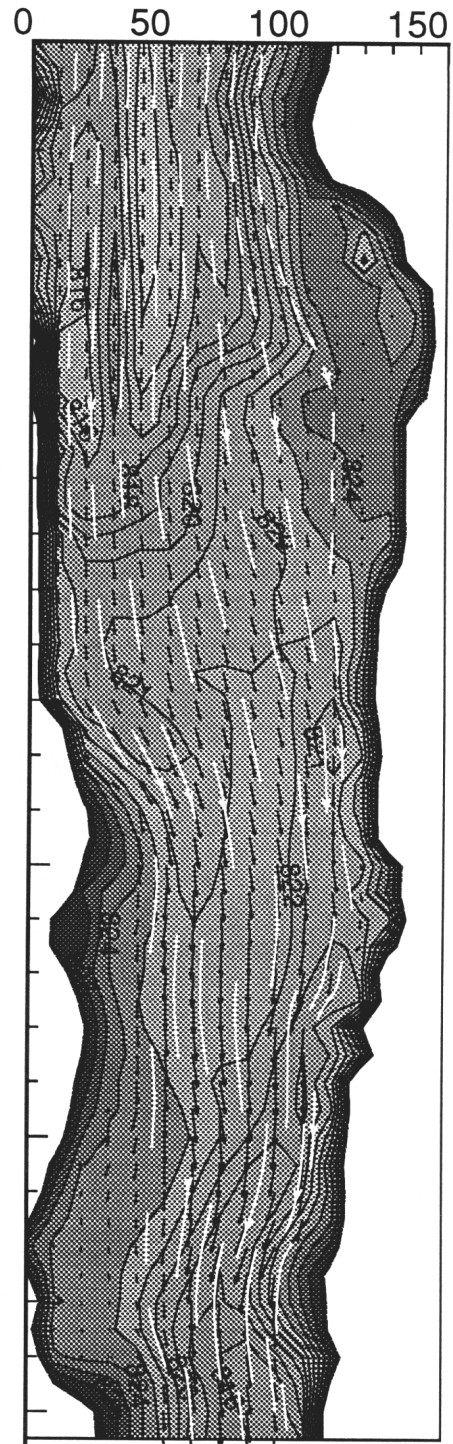
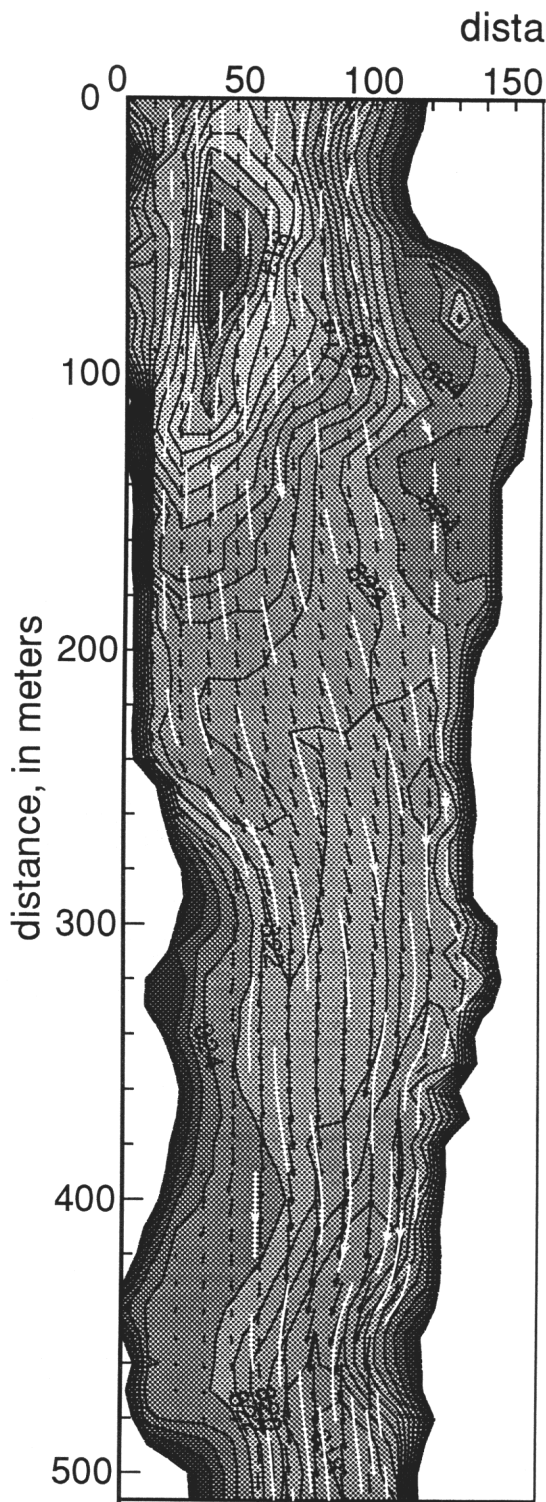


Fig 6



EXPLANATION

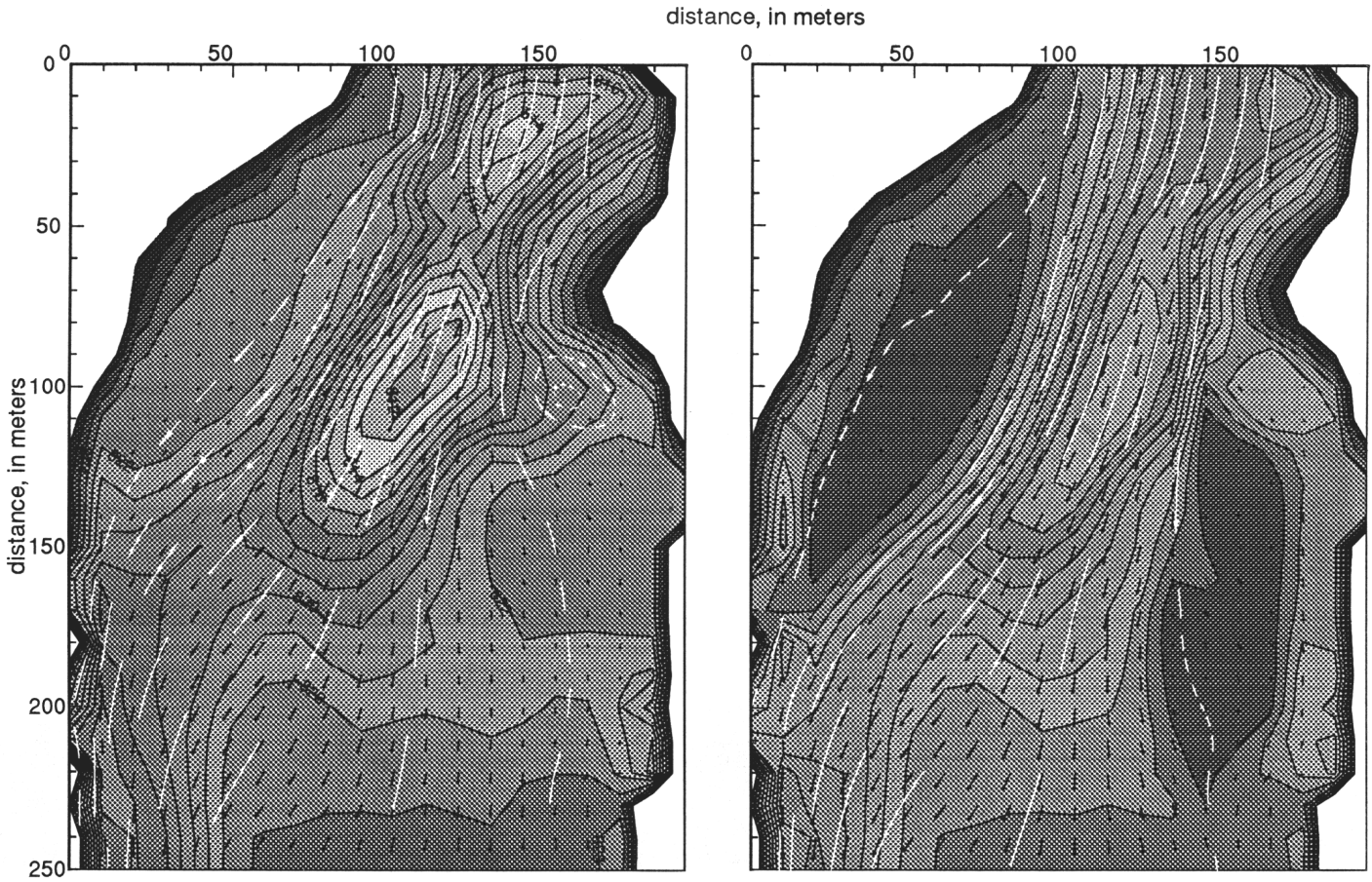
— 824 — CONTOUR—Interval 1 meter. Datum is mean sea level

— VELOCITY VECTOR—Length is proportional to velocity magnitude

— STREAMLINE



Fig 7



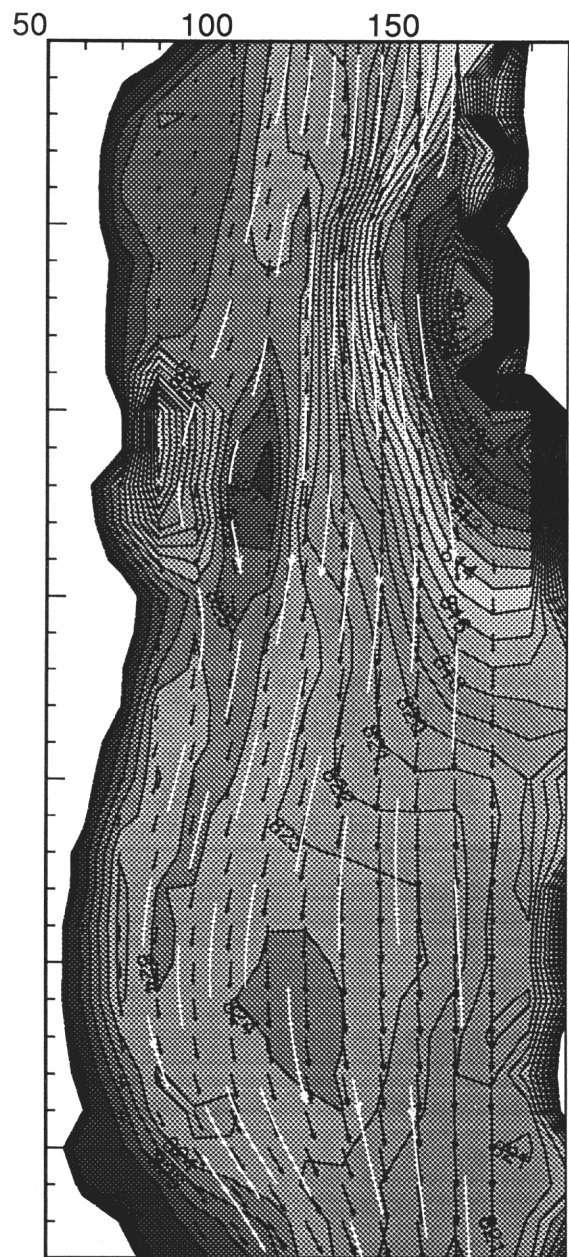
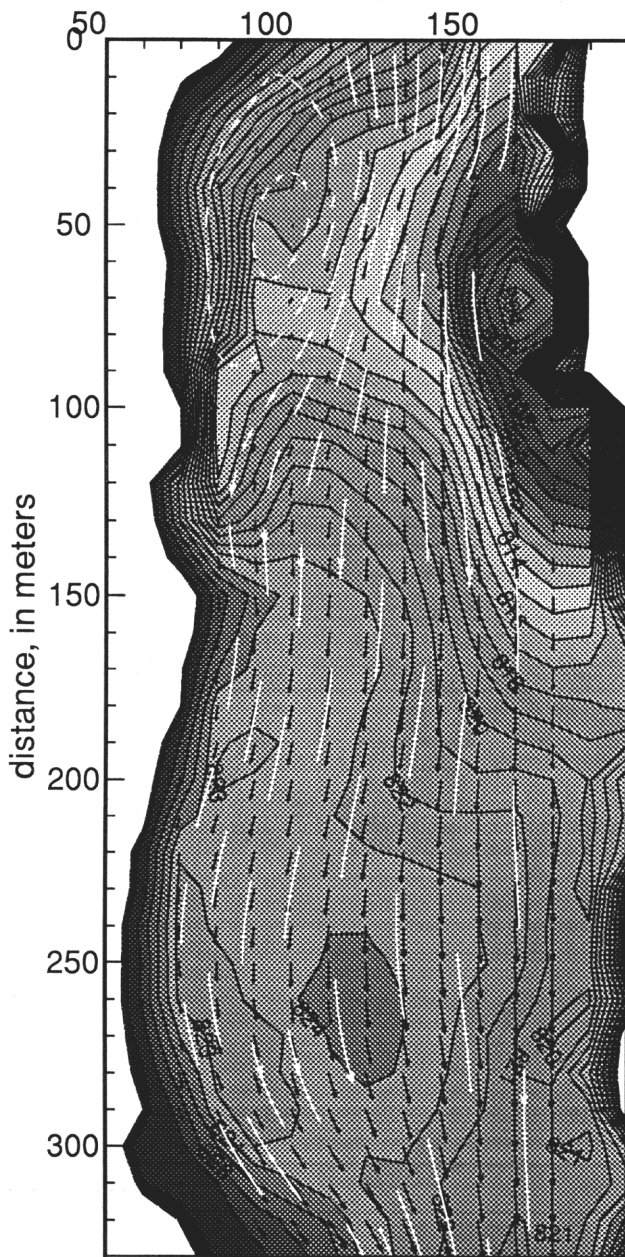
EXPLANATION

<p>— 1 m — CONTOUR—Interval 1 meter. Datum is mean sea level</p> <p>→ STREAMLINE</p>	<p>→ VELOCITY VECTOR—Length is proportional to velocity magnitude</p>
--	---



Fig 8

distance, in meters

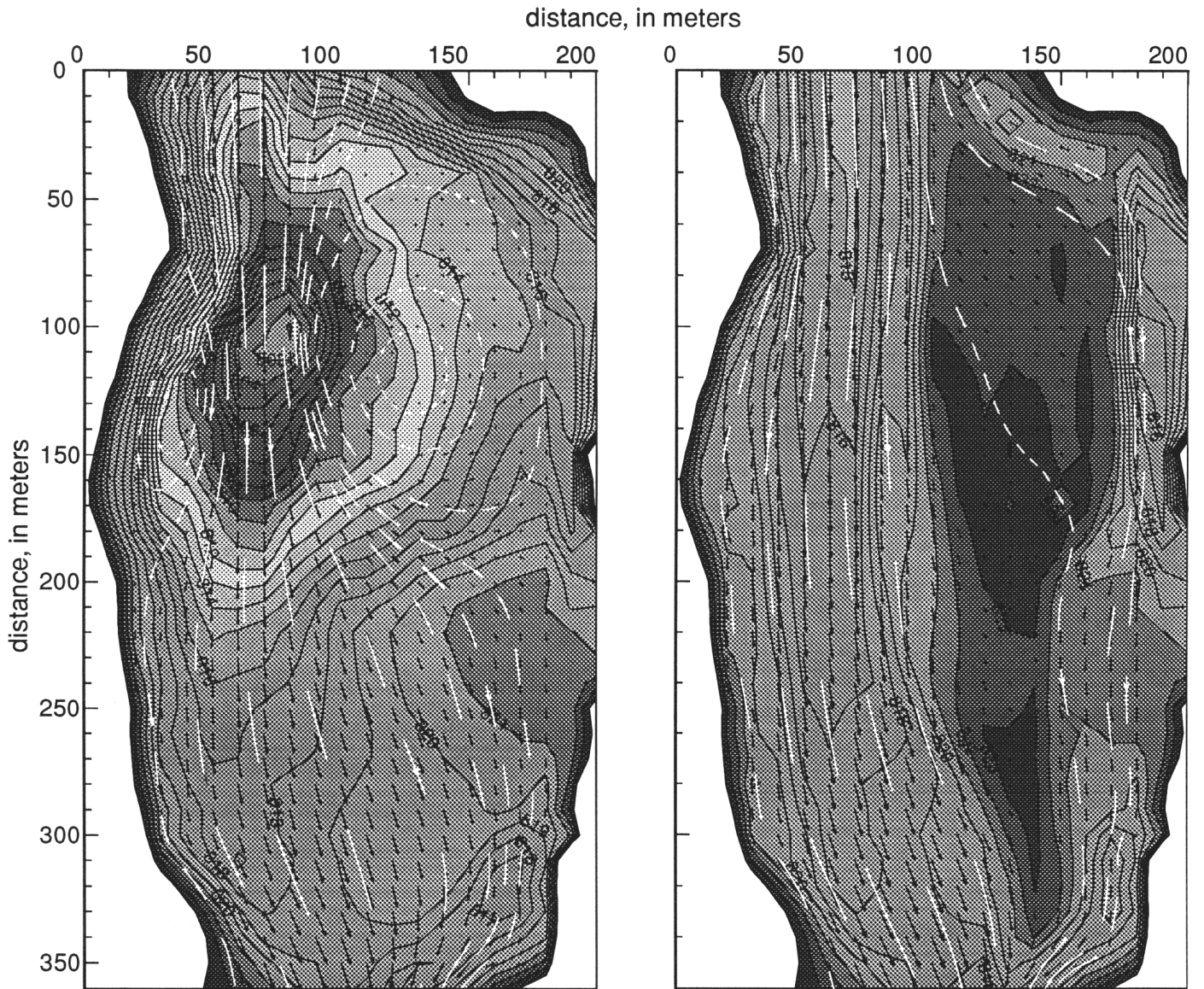


EXPLANATION

- 818 - CONTOUR—Interval 1 meter.
Datum is mean sea level
- VELOCITY VECTOR—Length is
proportional to velocity magnitude
- STREAMLINE



Fig 9



EXPLANATION

<p>— 818 — CONTOUR—Interval 1 meter. Datum is mean sea level</p> <p>→ STREAMLINE</p>	<p>→ VELOCITY VECTOR—Length is proportional to velocity magnitude</p>
--	---



Fig 10

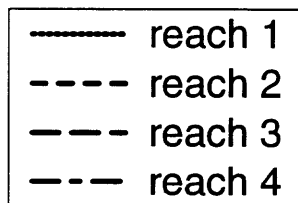
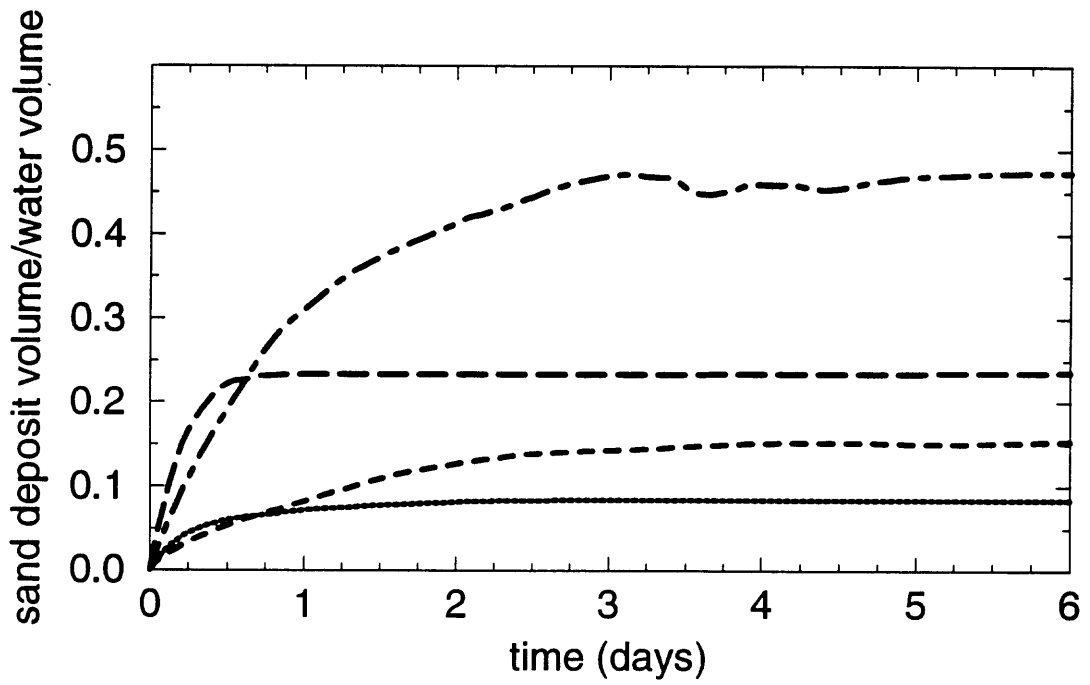
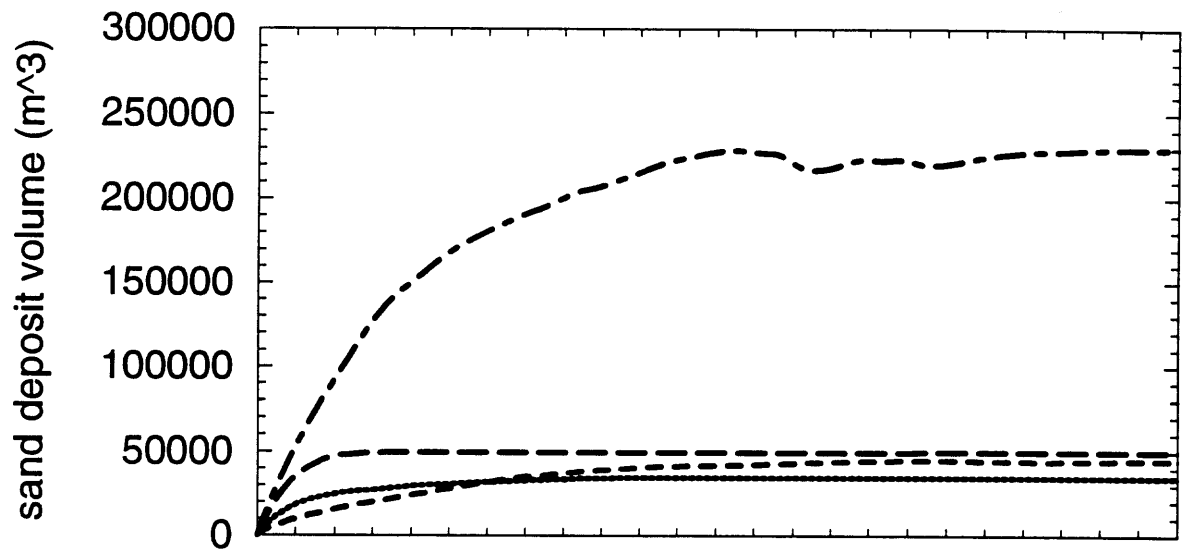


Fig 11

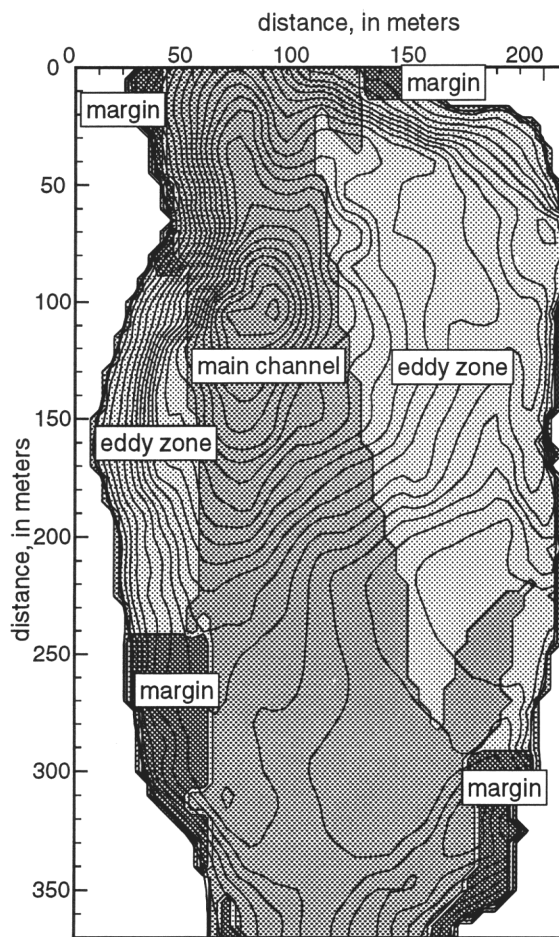


Fig 12

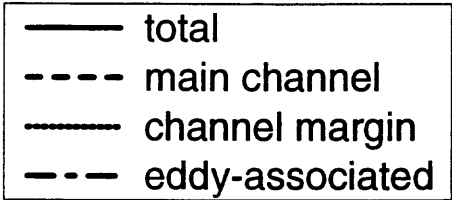
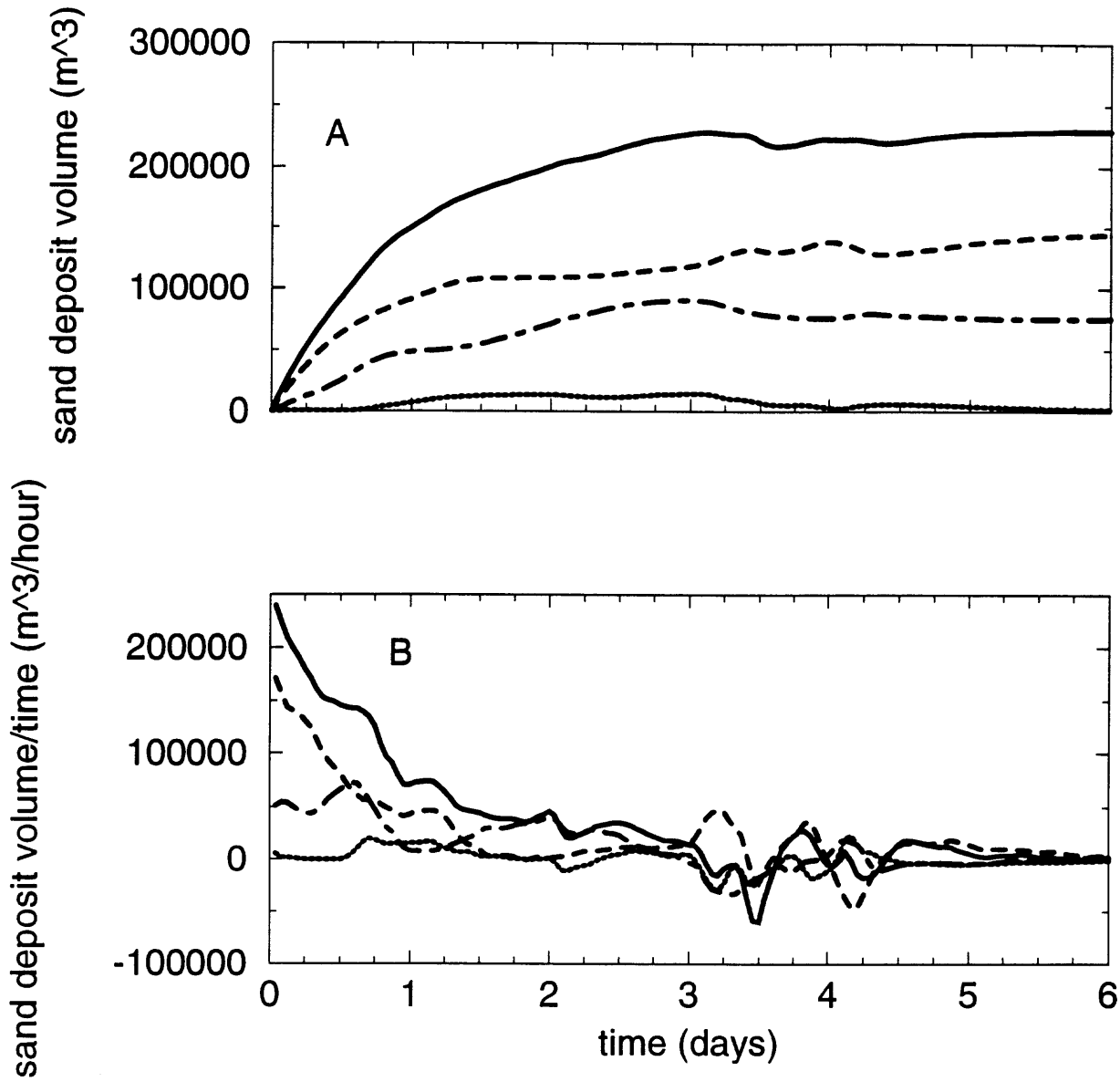


Fig 13

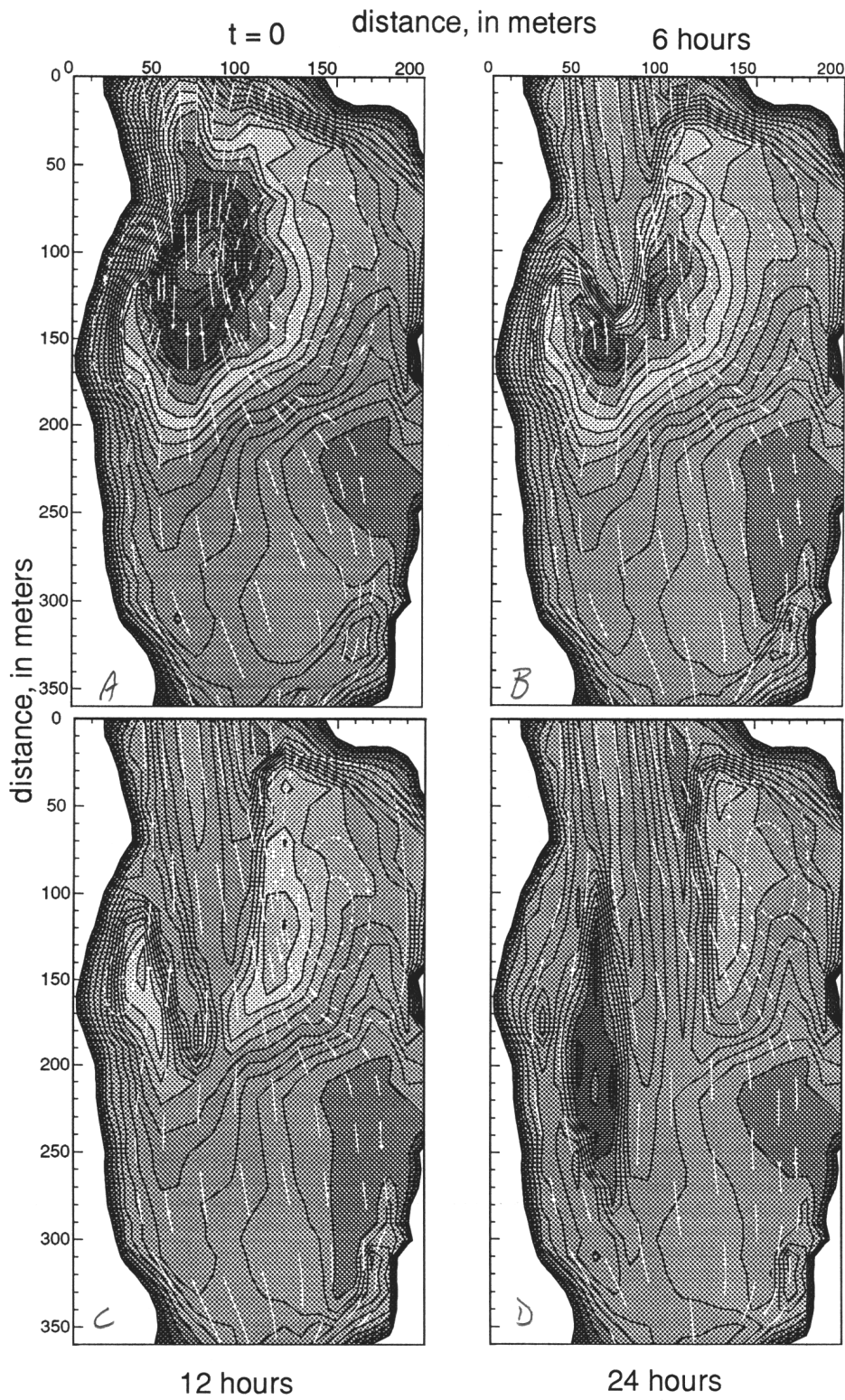


Fig 14

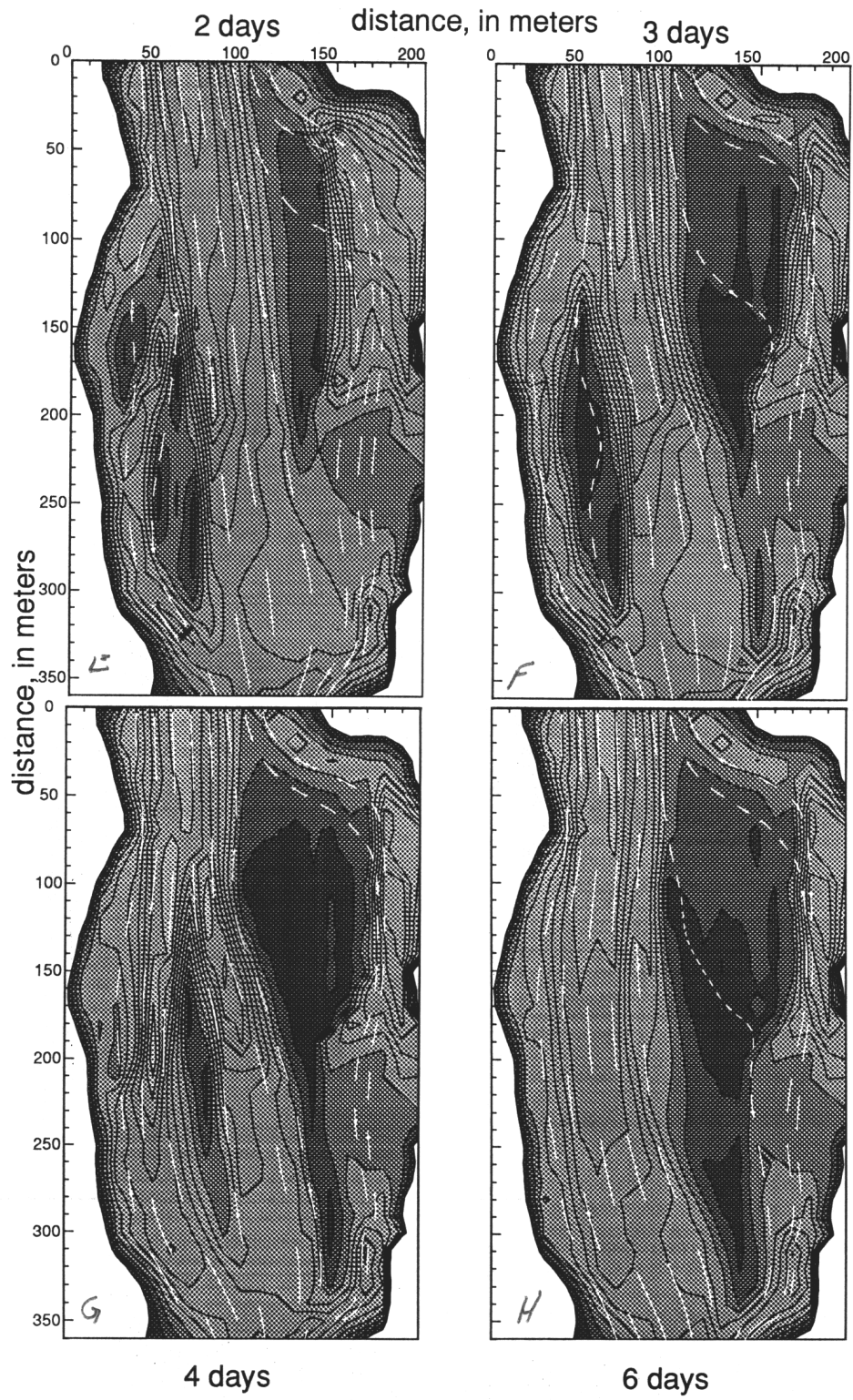


Fig 14 cont'd